ELSEVIER

International Journal of Mass Spectrometry 218 (2002) 131–160

International Journal of Mass Spectrometry

www.elsevier.com/locate/ijms

Gas phase ion chemistry of *para* substituted benzene diazonium ions, their salt clusters and their related phenyl cations

Ana K. Vrkic, Richard A.J. O'Hair*

School of Chemistry, University of Melbourne, Melbourne, Vic. 3010, Australia

Received 14 December 2001; accepted 30 March 2002

Abstract

Electrospray ionization of the tetrafluoroborate salts of *para* substituted (chloro, bromo, nitro and methoxy) benzene diazonium ions ($XC_6H_4N_2^+$ where X = Cl, Br, NO_2 and CH_3O) results in the formation of the bare diazonium ion as well as the mixed inorganic/organic salt ions $[XC_6H_4N_2^+(XC_6H_4N_2^+BF_4^-)_n]$ in the positive ion mode and the bare tetrafluoroborate anion and salt ions $[BF_4^-(XC_6H_4N_2^+BF_4^-)_n]$ in the negative ion mode. Tandem mass spectrometry (MS/MS) experiments were carried out on $XC_6H_4N_2^+$, $[XC_6H_4N_2^+(XC_6H_4N_2^+BF_4^-)_n]$ and $[BF_4^-(XC_6H_4N_2^+BF_4^-)_n]$ ions. ESI/MS and ESI/MS/MS data are presented which provide some support for "magic number" salt clusters observed for each of the four diazonium salts. Collision induced dissociation of $XC_6H_4N_2^+$ ions result in the formation of highly reactive phenyl cations, $XC_6H_4^+$ in all cases. The gas phase reactivity of both $XC_6H_4N_2^+$ and $XC_6H_4^+$ ions towards nine different nucleophiles, NuY (where NuY = H_2O, CH_3OH, CD_3OD, CH_3CN, $(CH_3)_2CO$, $(CD_3)_2CO$, $CH_3C(O)NHCH_2CH_3$, pyrrole and aniline) was examined using a quadrupole ion trap mass spectrometer. While the diazonium ions were generally unreactive towards these nucleophiles, the phenyl cations readily react to yield the energized adducts ($XC_6H_4NuY^+$). These energized adducts undergo several different fragmentation reactions, including an unusual radical loss of the *para* substituent. The gas phase CID reactions of stabilized adducts ($XC_6H_4NuY^+$) were also examined and fragmented via similar types of reactions. Finally, the unusual radical loss of the *para* substituent from the adduct $O_2NC_6H_4NCCH_3^+$ was shown to yield the distonic ion $C_6H_4NCCH_3^{\bullet+}$ via its $I^\bullet$ and $CH_2CHCH_2^\bullet$ radical abstraction reactions with allyl iodide. (Int J Mass Spectrom 218 (2002) 131–160)

Keywords: Aryl diazonium ions; Aryl cation; ESI/MS; Ion–molecule reactions; CID

1. Introduction

Interest in the reactivity of diazonium ions continues, with recent work focusing on their use as chemical probes of the interfacial compositions of micelles, microemulsions, reverse micelles and cyclodextrins [1a]. These studies rely on the fact that diazonium ions readily decompose via loss of N_2, both in solution and in the gas phase (Eq. (1)) [1b–d]. Dissociation of the benzene diazonium ion (X = H) requires only 27.3 kcal mol^{-1} in the gas phase (based upon the known heats of formation of PhN_2^+ (242 kcal mol^{-1}) and Ph^+ (269.3 kcal mol^{-1}) [2], which has been confirmed by ab initio calculations (which give a dissociation energy of 27.8 kcal mol^{-1}) (for ab initio studies on the structures of aryldiazonium ions see

* Corresponding author. E-mail: rohair@unimelb.edu.au

1387-3806/02/$ – see front matter
PII S1387-3806(02)00647-4

[3]). Understanding the mechanisms of the reactions of aryl diazonium ions in solution has been a challenge since they are very much dependent upon the reaction conditions, with some reactions proceeding via ionic pathways while others proceed via radical pathways [1]. Reaction conditions which favor ionic pathways include: attack at the terminal nitrogen atom (Eq. (2)); nucleophilic substitution of the N_2 group (Eq. (3)); and benzyne formation (Eq. (4)). The exact mechanism for substitution (Eq. (3)) has been a matter of lively debate, but is now thought to proceed via an ion–molecule complex between a phenyl cation and N_2 [1a].

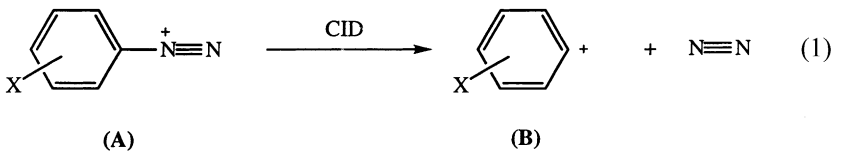

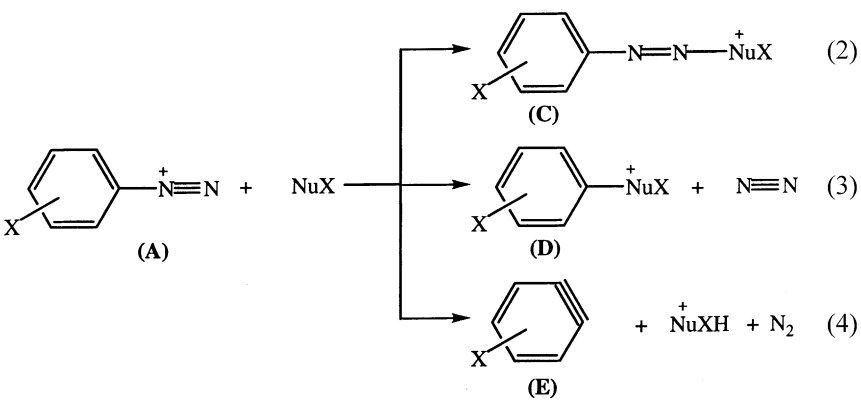

Examining the gas phase reactions of aryl diazonium ions and comparing their reactivity to the free aryl cations offers the opportunity to reveal their intrinsic reactivity. The gas phase chemistry of diazonium ions has received little attention [4], mainly due to a lack of methods for their gas phase synthesis. To date, the ion–molecule reactions of $CH_3N_2^+$ have been examined [4a], the heats of formation of $CH_3N_2^+$ [4b] and PhN_2^+ [4c] have been determined and CN_3^+ has been shown to be stable in the gas phase [4d]. More recently, Broxton et al. have shown that electrospray ionization can be used to transfer aryldiazonium ions from solution to the gas phase and that many of these diazonium ions can undergo collision induced dissociation to yield aryl cations via N_2 loss (cf. Eq. (1)) [4e,f]. By studying the fragmentation reactions as a function of collision energy, they were able to establish the relative stability order of eleven aryl diazonium ions [4e]. Similar investigations involving substituted 2-nitrobenzene diazonium cations revealed these species were less prone to N_2 loss relative to the monosubstituted cations [4f].

The gas phase reactions of free aryl cations have, in contrast, received more attention [5–8]. Thus, Speranza and coworkers have examined a wide array of aryl cation reactions under radiolytic conditions, [5] while others have examined ion–molecule reactions of aryl cations in triple quadrupole mass spectrometers, [6] ion cyclotron resonance mass spectrometers [7] and quadrupole ion-trap mass spectrometers [8]. Of most relevance to the work described here are the ion-trap reactions of the phenyl cation (**B**) (where X = H) with water, alcohols and amines which yield: adducts (Eq. (5)), products arising from dissociating adducts (Eq. (6)), abstraction reactions (Eq. (7)), deprotonation to yield benzyne (Eq. (8)), and electron transfer (Eq. (9)) [8].

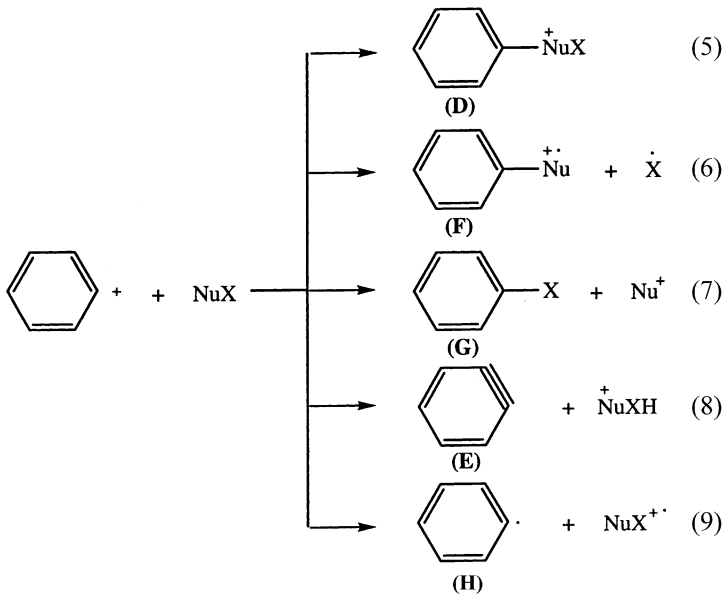

An important issue relevant to the gas phase reactivity of aryl cations (**B**), is their initial structure and the structure(s) of the resultant products arising from reactions with nucleophiles (e.g., (**D**)). Key papers which deal with these issues are briefly discussed below.

1.1. Structures of aryl cations: cyclic vs. acyclic structures

The parent phenyl cation ((**B**), where X = H) has been most extensively studied. Several theoretical studies have examined the relative stabilities of a range of isomeric $[C_6H_5]^+$ structures [9]. Early molecular orbital studies [9a–d], focused on determining whether the phenyl cation existed in its singlet state (having a vacant sp^2 orbital orthogonal to the π system of the aromatic ring) or as the triplet biradical (involving transfer of a π electron from the benzene ring into the vacant sp^2 orbital, accompanied by spin inversion). In all instances, the molecular orbital calculations predicted the ground state of the phenyl cation to be a singlet. A more recent study has involved performing ab initio molecular orbital calculations for the phenyl cation, phenyl radical and the phenyl anion and once again found the ground state of the phenyl cation to be a singlet [9e]. Tasaka et al. [9f] investigated 14 possible isomeric forms of the $C_6H_5^+$ system and found the singlet phenylium ion to have the lowest energy, with the acyclic isomers possessing much higher heats of formation.

Generation of isomerically pure populations of the phenyl cation in the gas phase has been reported in a number of studies, some of which include spontaneous, β^- decay of suitably multitritiated benzenes [5a], chemical ionization of halobenzenes with Brønsted acids [7a] and CID MS/MS of the molecular ion of chlorobenzene [8]. Ausloos et al. used ion–molecule reactions with hydrocarbons and polar molecules to probe the formation of ground-state phenyl cations in low energy processes and showed that higher-energy acyclic $[C_6H_5]^+$ ions appeared upon high-energy electron impact fragmentation of C_6H_6 and halobenzenes [7b]. A recent study by Nelson and Kenttamaa also showed that both the cyclic and acyclic isomers of the related 3,5-didehydrophenyl cation could be generated, and that these isomers could be distinguished via ion–molecule reactions [10]. Schroder et al. have shown that a different experimental technique (charge reversal ($^+CR^-$) of cations to anions) can be used to structurally differentiate isomeric $[C_6H_5]^+$ ions [11].

1.2. Structures of aryl cations: retention of the position of the substituent relative to the charge site

An important question in any study involving aryl cations is "once an aryl cation is synthesized does it retain the position of charge relative to any substituents on the ring, or does it undergo an intramolecular rearrangement?" One of the simplest isomerization reactions involves automerization in which the charge site migrates via a 1,2 hydride shift as shown in Eq. (10). Recent theoretical estimates suggest that the aryl cation would need to be formed with considerable excess energy in order to overcome the barrier for this reaction [12]. Relevant thermochemical data for three systems is shown under Eq. (10) and in all cases the barrier is over 46 kcal mol^{-1}. Thus in processes where the aryl cation is formed with little excess energy, this automerization is unlikely to occur.

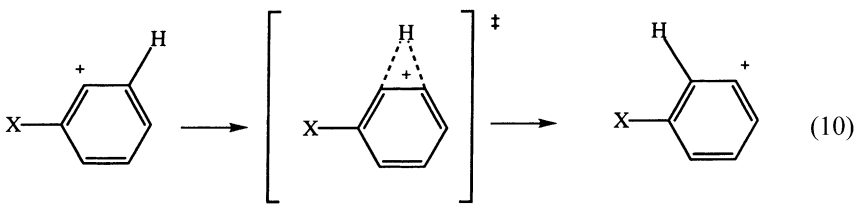

(10)

$X = H$; $\Delta H^{\circ} = 0$ kcal mol^{-1}; $\Delta H^{\ddagger} = +47.2$ kcal mol^{-1}
$X = CH_3$; $\Delta H^{\circ} = +1.6$ kcal mol^{-1}; $\Delta H^{\ddagger} = +46.8$ kcal mol^{-1}
$X = SiH_3$; $\Delta H^{\circ} = +6.4$ kcal mol^{-1}; $\Delta H^{\ddagger} = +53.8$ kcal mol^{-1}

Decay of uniformly multitritiated species yields isomeric aryl cations $XC_6H_4^+$ (X = NO_2, CN, Cl, Br, OH and OCH_3) formed in initial 2:2:1 relative yields of *ortho*:*meta*:*para*. The gas phase intramolecular isomerization reactions of these aryl cations can be evaluated by examining the products of their ion–molecule reactions with methanol (which yield the isomeric substituted anisoles upon deprotonation) and methyl halides (which yield the isomeric substituted aryl halides) [5b]. The only systems which give substantial changes from the expected 2:2:1 distributions of *ortho*:*meta*:*para* isomer products occur for the aryl cations $XC_6H_4^+$ (X = NO_2, OH and OCH_3). Depletions in the *ortho* products when X = NO_2 and OCH_3 were attributed to intramolecular electron transfer for X = NO_2 and intramolecular hydride transfer from the methoxy group for X = OCH_3. In contrast, depletion of the *meta* isomer for X = OH was attributed to a bimolecular proton transfer to give a cumulene like structure.

1.3. Structures of the products arising from reactions between aryl cations and nucleophiles

The final complication that can yield a different product isomer to that expected is that the initially formed product can undergo intramolecular isomerization or isomerization induced by an ion–molecule reaction with another neutral (e.g., via proton transport catalysis [13]). Give the importance of the reactivity of aryl cations, it is surprising that there are few detailed theoretical studies of the potential energy surfaces of their reactions with nucleophiles. An exception is a recent detailed DFT study on the reactions of the phenyl cation with methanol and methyl fluoride [14]. These workers found that of the four potential ways in which the phenyl cation could interact with methanol (i.e., addition to the oxygen lone pair or insertion into either the CO, CH or OH bonds), the *O*-protonated anisole addition complex was found to be lowest in energy. This was in contrast to the DFT results in the phenyl cation-methyl fluoride system, which showed that insertion into the CF bond was most stable. These DFT calculations

demonstrated that addition and insertion processes are all significantly exothermic (>33 kcal mol^{-1}) and that the initially formed products have sufficient energy to isomerize via intramolecular H migration (which have barrier heights in the 1–23 kcal mol^{-1} range) and CH_3 migration (which have barrier heights in the 5–28 kcal mol^{-1} range). Overall, the global minima were found to be *para*-protonated anisole and *meta*-protonated *ortho*-fluorotoluene.

As noted above, adducts of the type $C_6H_5YH^+$ are often less stable than their ring protonated isomers and are thus potentially susceptible to isomerization reactions. For example, the water adduct (*O*-protonated phenol) is not as stable as the *para* ring protonated isomer [15,16]. This trend is also apparent in various halogenated phenols, X–C_6H_4–OH (X = H, F, Cl, Br, I) since a theoretical study has shown that for the *ortho* and *meta* halogenated phenols, the most favored site of protonation was *para* to the OH substituent [15a]. Other systems in which the issue of ring vs. substituent protonation have been discussed include protonated isopropyl phenyl ether [17a] and *N*-alkylanilines [17b].

Given the inherent limitations of providing unequivocal structural assignments due to the isomerization reactions discussed above, many of the schemes and equations presented in this paper assume that the *para* positional relationship between the substituent and the diazonium group is retained for the charge site location in the aryl cation and in its ion–molecule reaction products. In some instances, further experiments have been carried out in an attempt to confirm structures. In other cases, such experiments have not been possible and the formation of other isomers remains a distinct possibility.

In this paper we discuss the: (i) formation of salt cluster ions of tetrafluoroborate salts of diazonium ions; (ii) the gas phase ion molecule reactions of the diazonium ions (**A1**–**A4**); (iii) the gas phase ion molecule reactions of free aryl cations (**B1**–**B4**); (iv) gas phase fragmentation reactions of some of the adducts formed via Eq. (5); (v) ion–molecule reactions as a probe of the formation of novel aryl distonic ions of the type $C_6H_4NCCH_3^+$.

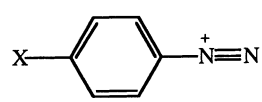

(A1) X = Cl
(A2) X = Br
(A3) X = NO_2
(A4) X = CH_3O

(B1) X = Cl
(B2) X = Br
(B3) X = NO_2
(B4) X = CH_3O

2. Experimental section

All experiments were performed using a commercially available quadrupole ion trap mass spectrometer (Finnigan-MAT model LCQ, San Jose, CA) equipped with electrospray ionization (ESI) and recently modified to allow the introduction of neutral reagents via the helium background gas inlet line [18]. All reagents except those described below were commercially available and used without further purification.

The diazonium salts were synthesized via standard literature procedures and were isolated as their tetrafluoroborate salts [1c]. The diazonium salts were dissolved in a 50:50 mixture of CH_3CN and CH_3OH (0.1 mg/mL) and were introduced to the mass spectrometer at 3.0 μL/min via electrospray ionization. Typical ESI conditions used were: spray voltage, 4.5–5.5 kV, capillary temperature, 200 °C, nitrogen sheath pressure, 30 psi, and capillary voltage, 0–10 V. The diazonium ions were very sensitive to fragmentation via loss of N_2 in the gas phase. We found that optimizing the tube lens offset voltage was one of the key variables to observing gas phase diazonium ions. Once a stable signal was obtained, the neutral reagents were introduced into the trap as a part of the helium bath gas. A constant flow of the reagent (30 μL/h) was established using a syringe pump with the syringe's needle being directed into a measured flow of helium (100–1500 mL/min). Rapid vaporization at the needle under these conditions allows for molar mixing ratios of ∼10^3–10^5 (He/reagent). The majority of the gas exits through a flowmeter, whereas a small amount (∼1 mL/min) is drawn into the trap. The LCQ uses a constriction capillary to control the helium flow and is designed to maintain

1.75 mTorr in the trap when 3 psi of He pressure is applied to the capillary. In the stock system, the 3 psi is maintained by an internal regulator that steps down the 40 psi of He that is delivered at the external port. To avoid the dead volume in the internal regulator, we bypass it and deliver the He mixture (3 psi) directly to the capillary. This greatly decreases the lag time after changes in reagent concentration [19].

2.1. Synthesis of p-bromo-N-ethyl-acetanilide

Since this appears to be the first literature report of this compound, we describe its synthesis and characterization via ^{1}H and ^{13}C NMR and EI/MS, ESI/MS and High resolution MS below. A bromine solution (5.3 mL in 25 mL of glacial acetic acid) was added slowly and with constant shaking to a cooled (ice-bath) mixture of finely powdered *n*-ethylacetanilide (16.3 g, 0.1 mol) in 45 mL of glacial acetic acid. Once all the bromine was added, the solution remained an orange color due to a slight excess of bromine and a precipitate was observed. The final reaction mixture was allowed to stand at room temperature for 30 min with occasional shaking, and was then poured in 400 mL of water. The resultant mixture was stirred well and sodium metabisulphite solution was added until the orange color disappeared. The product was extracted with dichloromethane and upon evaporation of the solvent, yielded an oil. The *ortho*- and *para*- substituted products were separated by distillation, with boiling points of 114 and 121 °C/2 mmHg, respectively. The *para*-substituted product yielded crude crystals upon cooling which were recrystallized from ethanol, to yield red/brown crystals (3.5 g, 15%, m.p., 35–37 °C).

The spectroscopic data for *p*-bromo-*N*-ethyl-acetanilide are: (1) ^{1}H NMR spectrum ($CDCl_3$, 300 MHz, Varian Unity-300) which showed signals at δ 1.08 (t, 2H, C**H$_2$**CH$_3$), 1.81 (s, 3H, C(O)C**H$_3$**), 3.70 (q, 3H, CH$_2$C**H$_3$**), 7.05 (d, Ar 2H), 7.52 (d, Ar 2H). (2) ^{13}C NMR spectrum ($CDCl_3$, 300 MHz, Varian Unity-300) showed signals at δ 12.99 (CH$_2$**C**H$_3$), 22.74 (C(O)**C**H$_3$), 43.77 (**C**H$_2$CH$_3$), 121.62 (Ar **C**–Br), 129.87 (**C**H *ortho* to N), 132.85 (**C**H *ortho* to Br), 141.92 (Ar **C**–N), 169.58 (**C**(O)CH$_3$). (3) EI/MS (70 eV, direct insertion probe, Shimadzu GCMS-QP5050A) had ions (*m/z* 50 and above) at *m/z* 241/243 ($M^{\bullet+}$) (27%), 199/201 ($M^{\bullet+}$–$COCH_3$) (31%), 184/186 ($M^{\bullet+}$–$COCH_3$–CH_3) (100%), 70 ($CH_3CH_2NCCH_3^+$) (34%). (4) ESI/MS (Finnigan LCQ, 50:50 CH_3OH:CH_3CN) gave the major ion at *m/z* 242/244 [$(M + H)^+$] (100%). (5) High resolution data (Bruker BioApex 47e FT-ICR ESI/MS, 100% CH_3OH, direct infusion at 1 μL min^{-1}) showed abundant ions at 263.9991 (^{79}Br) (264.0000 theoretical) and 265.9968 (^{81}Br) (265.9979 theoretical) for the $[M + Na]^+$ ion corresponding to $C_{10}H_{12}NaNOBr$.

3. Results and discussion

3.1. ESI/MS of diazonium ions in the positive and negative ion mode

Electrospray ionization of tetrafluoroborate salts of aryl diazonium ions not only yields the diazonium ion (*p*-$XC_6H_4N_2^+$) in the positive ion mode and the tetrafluoroborate anion in the negative ion mode, but also yields charged salt clusters. In the positive ion mode these consist of (*p*-$XC_6H_4N_2^+$ $BF_4^-)_nXC_6H_4N_2^+$ clusters while in the negative ion mode, they consist of (*p*-$XC_6H_4N_2^+BF_4^-)_nBF_4^-$ clusters. We can only find one previous report on the formation of related clusters of the type $(ArN_2^+X^-)_nArN_2^+$ (n = 1, 2) via FAB/MS [20]. Fig. 1 shows the positive clusters formed for (A) X = Cl; (B) X = Br; (C) X = NO_2 and (D) X = CH_3O, while Fig. 2 shows the negative clusters formed for (A) X = Cl; (B) X = Br; (C) X = NO_2 and (D) X = CH_3O. It is interesting to note that much larger sized clusters are observed in these ESI experiments than those reported via FAB/MS [20].

There has been considerable recent interest in cluster ions formed via ESI, including those formed from simple inorganic salts [21a–c] and simple zwitterionic species [21c–f]. Apart from potential uses such as calibration ions for mass spectrometers [22], several studies have examined the fragmentation behavior of such systems and have looked for "magic numbers" which might provide indirect information

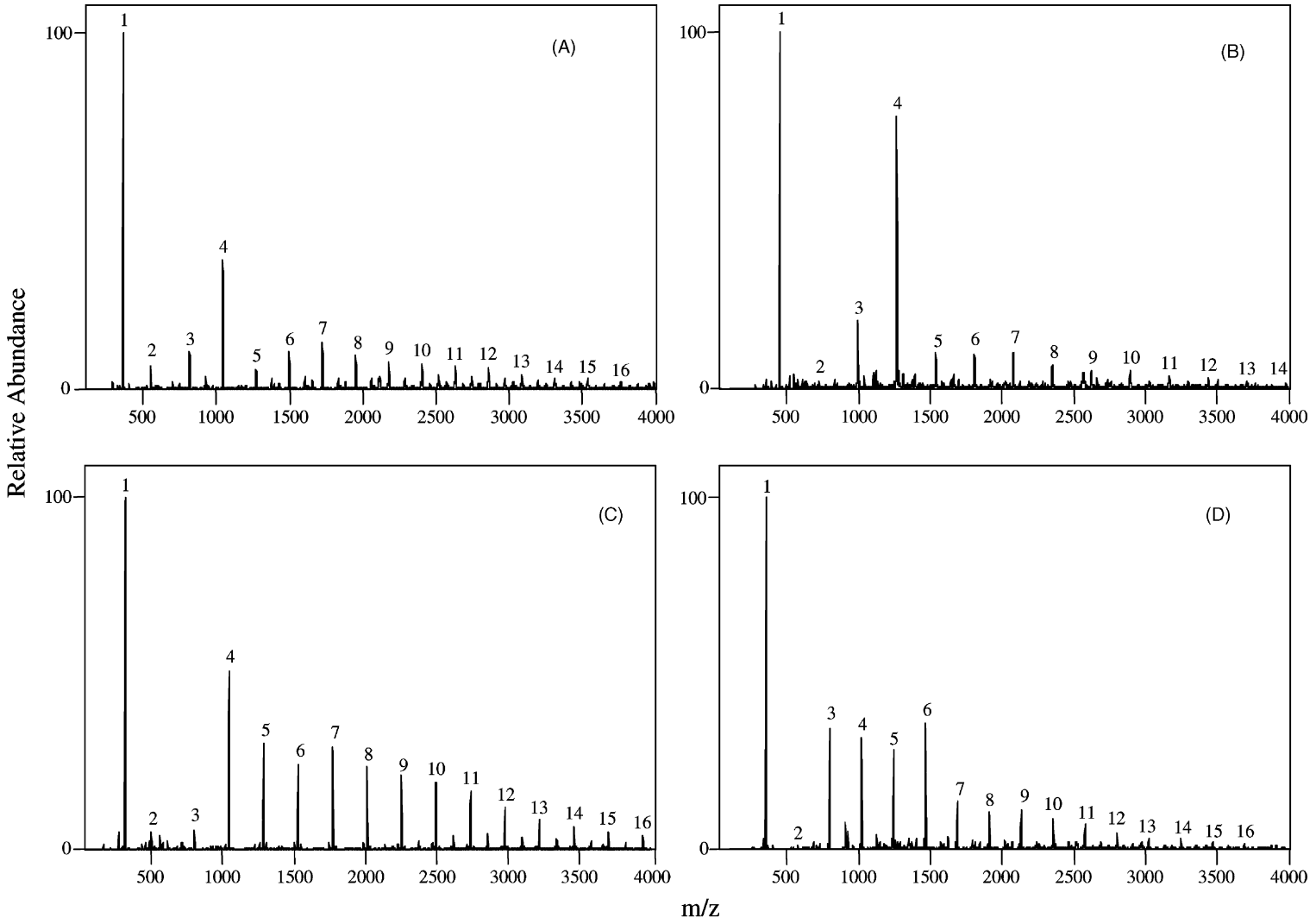

Fig. 1. ESI/MS of the *para*-X-phenyl diazonium tetrafluroroborate salt in the positive ion mode where X = (A) Cl, (B) Br, (C) NO_2 and (D) OCH_3.

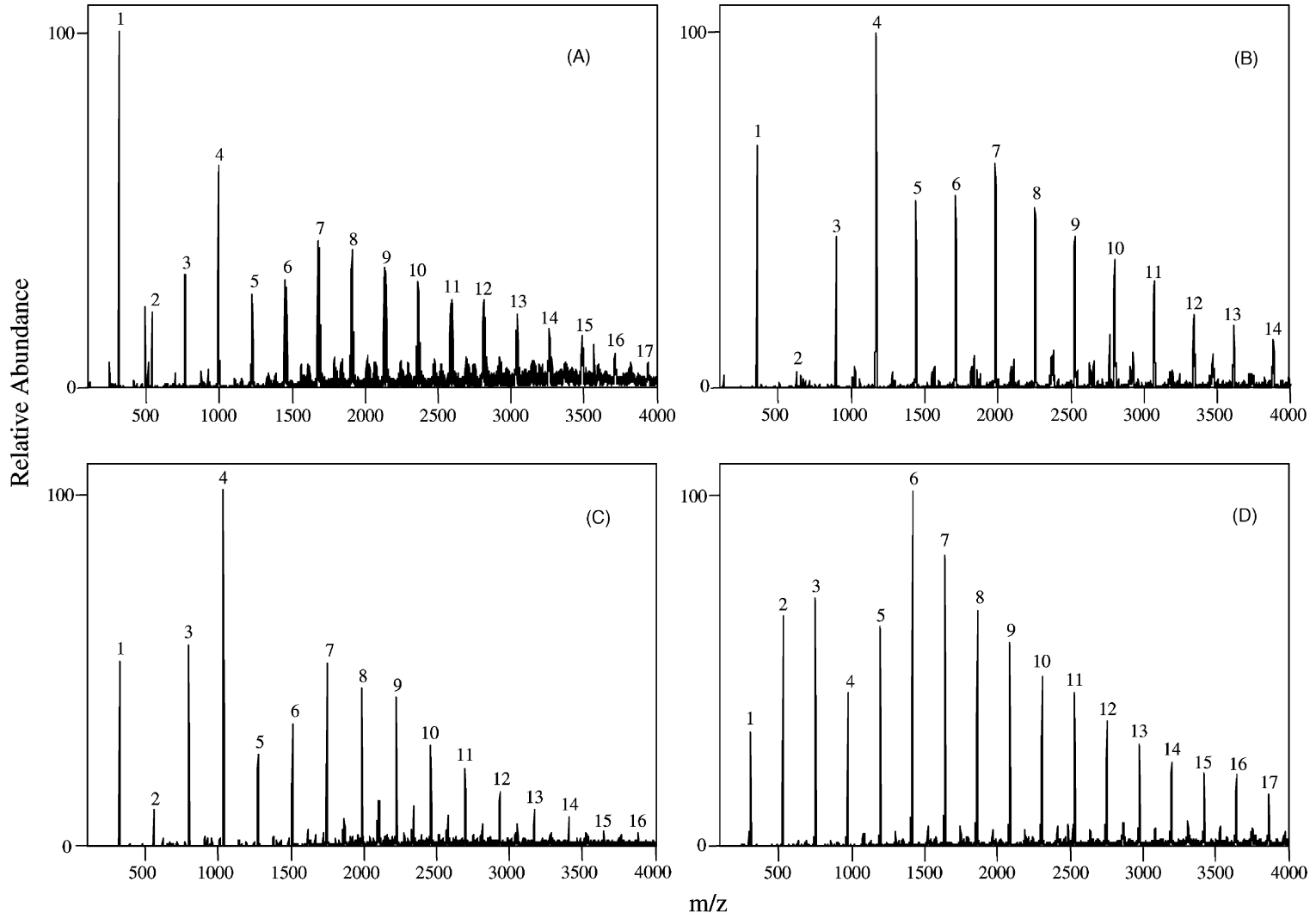

Fig. 2. ESI/MS of the *para*-X-phenyl diazonium tetrafluroroborate salt in the negative ion mode where X = (A) Cl, (B) Br, (C) NO_2 and (D) OCH_3.

on the gas phase structures of these cluster ions. Recently, Zhang and Cooks reported magic numbers for doubly charged sodium chloride cluster ions $[NaCl)_m(Na)^{2+}]^{2+}$ at $m = 11$, 12, 17, 20, 21, 26, 30, 34, 36, 44, 54 and 61, while Ince et al. observed magic numbers for $(NaF)_nNa^+$ and $(NaF)_mNa_2^{2+}$ clusters at $n = 4$, 7, 13, 22, 28, 31 and 37 and at $m = 11$, 12, 17, 20, 21, 30, 34 and 36, respectively [21a,b]. Both suggested these clusters ions take on the properties of close-packed cuboidal lattice structures, e.g., $n = 4$, 7 may assume $3 \times 3 \times 1$ and $3 \times 5 \times 1$ structures.

These studies also examined the influence of sample concentration and ESI conditions on the ion intensities/distributions of clusters. It was shown that low salt concentrations and high heated capillary temperatures (>200 °C) favored singly charged sodium chloride cluster ions. Thus, at high capillary temperatures, doubly charged sodium fluoride clusters were not favored and only stable sodium fluoride clusters which were not susceptible to decomposition after complete desolvation were observed. In our work, we have employed low salt concentrations and a "high" capillary temperature of 200 °C, resulting in the formation of the abundant singly charged cluster ions as shown in Figs. 1 and 2.

Figs. 1 and 2 reveal some evidence of "magic numbers," i.e., clusters whose ion intensities are greater than those of neighboring clusters, suggesting a greater degree of stability. In the case of $(p\text{-}XC_6H_4N_2^+BF_4^-)_n XC_6H_4N_2^+$ and $(p\text{-}XC_6H_4N_2^+BF_4^-)_nBF_4^-$ where X = Cl, Br and NO_2 the key cluster ions were at $n = 1$ and 4, while for X = CH_3O, the most important cluster ions were at $n = 1$ and 6. To determine whether the clusters formed in this gas phase study reflect the types of structures observed in the solid state, the published X-ray structures of $C_6H_5N_2^+BF_4^-$, $p\text{-}BrC_6H_4N_2^+BF_4^-$ and $p\text{-}O_2NC_6H_4N_2^+BF_4^-$ were viewed [23a–c]. In all three instances, the distribution of the tetrafluoroborate salts corresponded to close packed molecular chains and differed only by the number of cation interactions with surrounding anions. The distribution of the molecules in the crystal lattice of $C_6H_5N_2^+BF_4^-$ showed both nitrogens from the benzene diazonium cations in contact with one fluorine atom from each of four surrounding BF_4^- anions (<3.1 Å). Packing within $p\text{-}O_2NC_6H_4N_2^+BF_4^-$ was hampered by disordering of the anion. Nonetheless, there appeared to be interactions between each of the N_2 groups and three fluorine atoms from each of three surrounding BF_4 anions. The crystal structure of $p\text{-}BrC_6H_4N_2^+BF_4^-$ revealed the molecules conformed to molecular close packing, with the anions connected to surrounding cations by van der Waals forces. One very close contact between the azo nitrogens and a fluorine from the surrounding anion suggested it could be a weak ionic bond (2.81 Å for both). Given this evidence for weak ionic bonding between the N_2 group and the BF_4^- ion, we are able to suggest some possible structures (1–2), for the formation of the stable clusters at $n = 1$ for $(p\text{-}XC_6H_4N_2^+ BF_4^-)_n XC_6H_4N_2^+$ and $(p\text{-}XC_6H_4N_2^+BF_4^-)_nBF_4^-$ where X = Br and NO_2. A possible structure of the cluster ions at $n = 4$ may arise from two of either of the dimeric subunits 3 and 4 surrounding a core ion such as $p\text{-}XC_6H_4N_2^+$ or BF_4^-. Positions for the core ions are indicated by arrows on structures 3 and 4.

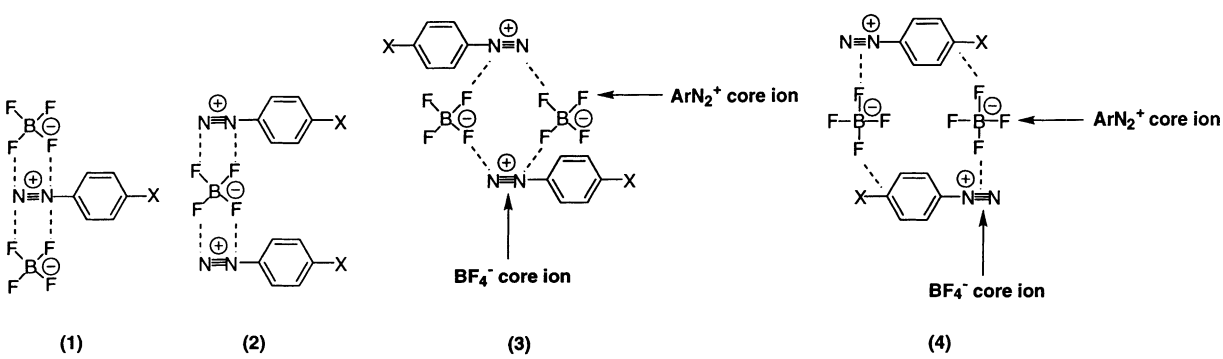

Table 1
LCQ CID MS/MS of $(4\text{-}BrC_6H_4N_2^+BF_4^-)_n$ $4\text{-}BrC_6H_4N_2^+$

Species selected (n)	Activation energy	CID products (n)					
		0	1	2	3	4	5
1	0.64	100	–	–	–	–	–
2	0.7	0	100	–	–	–	–
3	0.8	0	100	3	–	–	–
4	0.96	0	32	15	100	–	–
5	0.85	0	0	0	16	100	–
6	0.95	0	0	0	2	100	11

Table 3
LCQ CID MS/MS of $(4\text{-}BrC_6H_4N_2^+BF_4^-)_nBF_4^-$

Species selected (n)	Activation energy	CID products (n)					
		0	1	2	3	4	5
1	0.9	100	–	–	–	–	–
2	0.6	0	100	–	–	–	–
3	0.65	0	100	29	–	–	–
4	0.85	0	14	95	100	–	–
5	0.9	0	0	2	50	100	–
6	0.98	0	0	1	2	100	43

The difference between structures 3 and 4 is that only in structure 4 is there weak ionic bonding between the F and the *para* carbon atom. This type of interaction may become more important for electron withdrawing (X) substituents. To gain further information on the stability and fragmentation behavior of cluster ions, we have carried out CID on a limited range of these systems i.e., $(p\text{-}XC_6H_4N_2^+BF_4^-)_nXC_6H_4N_2^+$ (Tables 1 and 2) and $(p\text{-}XC_6H_4N_2^+BF_4^-)_nBF_4^-$ (Tables 3 and 4) clusters ions where X = Br and CH_3O.

Turning our attention to Table 1 we see that while there can be more than one fragmentation pathway for $(p\text{-}BrC_6H_4N_2^+BF_4^-)_nBrC_6H_4N_2^+$, the principal dissociation pathway involves loss of $(p\text{-}BrC_6H_4N_2^+BF_4^-)_1$ for $n = 1$, 2, 4, 5 and loss of $(p\text{-}BrC_6H_4N_2^+BF_4^-)_2$ for $n = 3$ and 6. Upon closer examination we see that generally, the most abundant dissociation products consist of a magic number cluster composition, e.g., CID of $n = 5$, 6 yield $n = 4$ while CID of $n = 2$, 3 give $n = 1$. The activation energies can also provide an insight into the relative stabilities of the magic numbers. The activation energy, activation Q and activation time are three parameters within the software which allow us to specify collision processes. In these experiments, the activation Q/time were kept constant (i.e., 0.25 and 100 ms, respectively), while only the activation energy (which is a measure of the amplitude of the resonance excitation RF voltage applied to the end-caps (in volts)) was altered. While $n = 4$, 6 require activation energies of 0.96 and 0.95, respectively, to fragment, $n = 5$ only requires 0.85 to generate the magic number of $n = 4$. Similar analysis of the CID pathways of $(p\text{-}MeOC_6H_4N_2^+BF_4^-)_nMeOC_6H_4N_2^+$ shows that while there is no obvious major trend in the activation energies, the magic number cluster ions of $n = 1$ and 6 do seem to be the most abundant product ions closely followed by $n = 3$, 4 and 5. Examination of $(p\text{-}BrC_6H_4N_2^+BF_4^-)_nBF_4^-$ and $(p\text{-}MeOC_6H_4N_2^+BF_4^-)_nBF_4^-$ (Tables 3 and 4) yield similar results to those observed in the positive

Table 2
LCQ CID MS/MS of $(4\text{-}MeOC_6H_4N_2^+BF_4^-)_n$ $4\text{-}MeOC_6H_4N_2^+$

Species selected (n)	Activation energy	CID products (n)							
		0	1	2	3	4	5	6	7
1	0.65	100	–	–	–	–	–	–	–
2	0.7	0	100	–	–	–	–	–	–
3	1.03	0	100	31	–	–	–	–	–
4	0.8	0	1	5	100	–	–	–	–
5	1.3	0	2	2	54	100	–	–	–
6	1.05	0	0	0	6	35	100	–	–
7	1.05	0	0	0	1	1	9	100	–
8	1.3	0	0	0	1	5	10	100	95

Table 4
LCQ CID MS/MS of (4-$MeOC_6H_4N_2^+BF_4^-$)$_n$$BF_4^-$

Species selected (n)	Activation energy	CID products (n)							
		0	1	2	3	4	5	6	7
1	0.6	100	–	–	–	–	–	–	–
2	0.65	0	100	–	–	–	–	–	–
3	0.65	0	0	100	–	–	–	–	–
4	0.73	0	0	77	100	–	–	–	–
5	0.85	0	0	16	75	100	–	–	–
6	0.97	0	0	16	20	68	100	–	–
7	1.15	0	0	1	8	7	25	100	–
8	1.2	0	<1	2	2	10	12	54	100

mode. CID of (p-$BrC_6H_4N_2^+BF_4^-$)$_n$$BF_4^-$ results in preferential formation of cluster species at $n = 1$ and 4, while CID of (p-$MeOC_6H_4N_2^+BF_4^-$)$_n$$BF_4^-$ gives magic numbers at $n = 6$, closely followed by $n = 2$, 3, 5 and 7, respectively.

3.2. Ion–molecule reactions of aryl diazonium ions, p-$XC_6H_4N_2^+$ (where X = Cl, Br, NO_2, OCH_3)

In order to determine the types of ion–molecule reactions that aryl diazonium ions undergo in the gas phase, we have examined the reactions of p-$XC_6H_4N_2^+$ (where X = Cl, Br, NO_2, OCH_3) with neutral nucleophiles ranging in basicity from water to aniline. The results of these experiments are shown in Table 5. In no case do any of these species undergo nucleophilic substitution (Eq. (3)) or benzyne formation (Eq. (4)). In some instances adduct formation is observed, however, assigning a structure for these adduct ions is difficult. In principle, they could be due to diazo formation (Eq. (2)) or they may simply be loosely bound ion–molecule complexes of the type (**I**). Attempts to mass select these ions and subject them to CID often proved difficult, and required a mass window of 10 Th. In those cases where CID was successful, only diazonium ion formation was observed.

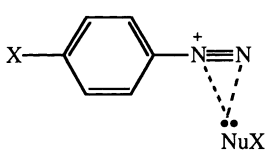

(**I**)

Although these are the first experimental results on the gas phase ion–molecule reactions of aromatic diazonium ions, Foster and Beauchamp have shown that the methyl diazonium ion readily undergoes substitution [4a]. The stark contrast between the reactivity of aromatic and aliphatic diazonium ions reflects the difference in nucleophilic substitution at a sp^2 hybridized vs. a sp^3 hybridized carbon atoms. Furthermore, our results are entirely consistent with some recent DFT calculations on the reaction between water and the phenyl diazonium ion which showed that even though the substitution reaction (Eq. (3)) is exothermic by some 7.3 kcal mol^{-1} at room temperature, there is a significant barrier of 28.5 kcal mol^{-1} relative to separated reactants [24]. Moreover, an initial complex of the type [$PhN_2^+(H_2O)$] is formed which is 11.8 kcal mol^{-1} more stable than the separated reactants. Thus if the systems studied here have similar barriers to reaction, they would not be expected to undergo reaction under the near thermal conditions of the ion trap [19]. At best they might form stabilized complexes of type (**I**) instead.

3.3. CID reactions of aryl diazonium ions, p-$XC_6H_4N_2^+$ in the presence of nucleophiles, and ion–molecule reactions of the resulting aryl cations, p-$XC_6H_4^+$ (where X = Cl, Br, NO_2, OCH_3) following N_2 loss

We have found the diazonium ions readily fragment via loss of N_2 in the gas phase, which is consistent with previous studies [4e,f]. This fragmentation can

Table 5
Ion–molecule reactions of *para* substituted diazonium 4-X–$C_6H_4N_2^+$ ions in the presence of nucleophiles

X	Neutral reagents, nucleophile	Products	
		Substitution reaction[a]	Adduct formation[b]
Cl	H_2O	–	–
	CH_3OH	–	–
	CD_3OD	–	–
	CH_3CN	–	–
	$(CH_3)_2CO$	–	9
	$(CD_3)_2CO$	–	<1
	$CH_3C(O)NHCH_2CH_3$	–	24
	Pyrrole	–	<1
	$C_6H_5NH_2$	–	<1
Br	H_2O	–	<1
	CH_3OH	–	–
	CD_3OD	–	–
	CH_3CN	–	–
	$(CH_3)_2CO$	–	<1
	$(CD_3)_2CO$	–	<1
	$CH_3C(O)NHCH_2CH_3$	–	21
	Pyrrole	–	<1
	$C_6H_5NH_2$	–	–
NO_2	H_2O	–	–
	CH_3OH	–	–
	CD_3OD	–	–
	CH_3CN	–	<1
	$(CH_3)_2CO$	–	<1
	$(CD_3)_2CO$	–	<1
	$CH_3C(O)NHCH_2CH_3$	–	100
	Pyrrole	–	<1
	$C_6H_5NH_2$	–	–
OCH_3	H_2O	–	–
	CH_3OH	–	–
	CD_3OD	–	–
	CH_3CN	–	<1
	$(CH_3)_2CO$	–	<1
	$(CD_3)_2CO$	–	<1
	$CH_3C(O)NHCH_2CH_3$	–	<1
	Pyrrole	–	–
	$C_6H_5NH_2$	–	<1

[a] Eq. (1).
[b] Abundance relative to parent diazonium ion.

be induced either in the tube lens region (i.e., before the diazonium ions are injected into the ion trap) by raising the tube lens offset voltage, or within the trap itself using standard excitation techniques. The resultant phenyl cations are highly reactive, readily intercepting any nucleophiles present. In order to examine the reactions of the phenyl cations, the parent diazonium ions were subjected to CID via tandem mass spectrometry (MS/MS) in the presence of H_2O, CH_3OH, CD_3OD, CH_3CN, $(CH_3)_2CO$, $(CD_3)_2CO$, $CH_3C(O)NHCH_2CH_3$, pyrrole and aniline (Table 6). Initial source CID involving the diazonium ions (p-XC_6H_4-N_2^+) was followed by mass selection of the substituted phenyl cations (p-$XC_6H_4^+$).

The MS/MS spectra show peaks from addition reactions of NuY (introduced through the helium line)

Table 6
CID reactions of *para* substituted diazonium 4-X–C_6H_4–N_2^+ ions in presence of nucleophiles

X	Nucleophile (Nu)	PA(Nu)[a]	IE(Nu)[a]	Products[b]
Cl[c]	H_2O	691	12.621	B(58); J(100); K(17); L(24); O(11); 93(57)
	CH_3OH	754.3	10.84	B(8); K(1); L(11); O(100)
	CH_3CN	779.2	12.2	B(1); L(100)
	$(CH_3)_2CO$	812	9.703	B(4); D(38); J(12); L(20); $(Nu + H)^+$ (34); O(11); 141(100); 151(7); 199(9)
	$(CD_3)_2CO$	–[d]	9.695	B(7); D(100); J(4); L(32); $(Nu + D)^+$ (7); $(Nu + H)^+$ (20); O(15); 143/145(48); 144/146(82); 157(10); 207(4); 208(7)
	$CH_3C(O)NHCH_2CH_3$	898	8.71	B(7); C(6); D(23); D + Nu(24); L(23); $(Nu + H)^+$ (40); $(2Nu + H)^+$ (100); 70(68)
	Pyrrole	875.4	8.207	B(9); C(2); D(7); J(2); L(13); $Nu^{\bullet +}$ (13); $(Nu + H)^+$ (4); O(1); R(100); 160(5)
	$C_6H_5NH_2$	882.5	7.72	B(14); D(31); L(29); $Nu^{\bullet +}$ (100); $(Nu + H)^+$ (27); R(92); 186(2)
Br, IE = 9.04	H_2O	691	12.621	B(6); J(53); K(100); L(19); O(11)
	CH_3OH	754.3	10.84	B(6); K(8); L(13); O(100); P(13)
	CH_3CN	779.2	12.2	B(1); J(1); K(3); L(100); O(2)
	$(CH_3)_2CO$	812	9.703	B(5); D(1); K(6); L(9); $(Nu + H)^+$ (2); O(5); R(100); R + Nu(6)
	$(CD_3)_2CO$	–[d]	9.695	B(4); D(4); K(7); L(10); $(Nu + H)^+$ (2); O(3); R(100); R + Nu(8)
	$CH_3C(O)NHCH_2CH_3$	898	8.71	B(8); C(11); D(26); D + Nu(30); L(30); $(Nu + H)^+$ (49); $(2Nu + H)^+$ (100); 70(66)
	Pyrrole	875.4	8.207	B(6); D(2); K(2); L(13); $Nu^{\bullet +}$ (21); $(Nu + H)^+$ (4); R(100)
	$C_6H_5NH_2$	882.5	7.72	B(13); D(31); J(2); L(29); $Nu^{\bullet +}$ (100); $(Nu + H)^+$ (30); O(1); R(92); 186(4)
NO_2, IE = 9.06	H_2O	691	12.621	B(<1); J(100); K(13); L(4); 123(2)
	CH_3OH	754.3	10.84	B(2); J(47); K(6); L(18); N(64); O(100); O + Nu(9); P(85); 137(15); 180(4)
	CH_3CN	779.2	12.2	B(<1); J(9); K(1); L(100); M(22); P(2); 133(11)
	$(CH_3)_2CO$	812	9.703	B(4); D(13); J(17); J + Nu (2); K(2); M(4); P(5); R(100); R + Nu(6); $(Nu + H)^+$ (13); 133(29); 163(23)
	$(CD_3)_2CO$	–[d]	9.695	B(<1); D(23); K(2); L(13); M(1); $(Nu + H)^+$ (9); P(4); R/J(100); R/J + Nu(9); 138(28); 169(7)
	$CH_3C(O)NHCH_2CH_3$	898	8.71	B(<1); C(15); D(23); D + Nu(60); J(2); $(Nu + H)^+$ (31); $(2Nu + H)^+$ (100); 70(19); 163(13); 250(4)
	Pyrrole	875.4	8.207	B(6); J(8); L(21); $Nu^{\bullet +}$ (100); $(Nu + H)^+$ (31); P (2); R(65); R + Nu(19); 131(8)
	$C_6H_5NH_2$	882.5	7.72	B(2); D(10); D + Nu(6); J(11); L(13); $Nu^{\bullet +}$ (100); $(Nu + H)^+$ (48); R(23)
OCH_3, IE = 8.32	H_2O	691	12.621	B(<1); J(100); L(6); O(5)
	CH_3OH	754.3	10.84	B(4); J(24); L(8); O(100)
	CD_3OD	–[d]	11	B(2); 110(2); 111(2); 124(49); 125(100); 126(9); L(7)
	CH_3CN	779.2	12.2	B(1); J(9); L(100); O(4)
	$(CH_3)_2CO$	812	9.703	B(6); D(100); D + Nu(2); J(30); J + Nu(2); L(16); $(Nu + H)^+$ (2); O(11); 105(23); 109(2); 137(23)
	$(CD_3)_2CO$	–[d]	9.695	B(2); D(100); J(21); J + Nu(2); L(13); $(Nu + H)^+$ (1); O(11); 139(30); 143(13)
	$CH_3C(O)NHCH_2CH_3$	898	8.71	B(2); D(100); D + Nu(52); L(37); $(Nu + H)^+$ (13); $(2Nu + H)^+$ (35); O(4); O + Nu(19); 70(75)

Table 6 (*Continued*)

X	Nucleophile (Nu)	PA(Nu)[a]	IE(Nu)[a]	Products[b]
	Pyrrole	875.4	8.207	B(4); D(100); J(15); L(12); $(Nu + H)^+$ (2); O(10); 159(13)
	$C_6H_5NH_2$	882.5	7.72	B(3); D(100); D + Nu(5); J(4); L(11); $Nu^{\bullet +}$ (17); $(Nu + H)^+$ (14); O(2); 168(4); 185(2)

[a] Energetics from NIST: PAs in kJ mol^{-1} and IEs in eV [2].
[b] Only products with 1% or greater relative abundance are listed.
[c] IE is unknown.
[d] PA is unknown, but is likely to be close to that of the unlabelled species.

as well as from the background gases H_2O, CH_3CN, CH_3OH (possible structures of ions which arise from the background gases include (**J**–**Q**), although other isomeric structures cannot be ruled out). Note that previous studies have shown that the LCQ has a significant background of water and ESI solvent molecules [18,25]. Not only are adducts observed (cf. Eq. (5)), but products due to fragmenting adducts are also observed (cf. Eq. (6)). This is entirely consistent with previous experimental studies on phenyl cations [5–8], as well as recent DFT calculations on the reaction between $C_6H_5^+$ and methanol [14], which have show that the high exothermicity of addition (-61.4 kcal mol^{-1} [14], -72.1 kcal mol^{-1} [8]) is sufficient to overcome many barriers for subsequent reactions of the energized adducts. Perhaps the most interesting reaction arises from cleavage of the *para* X–C bond (Eq. (11)) which may result in the formation of a distonic ion. Although such a reaction has not been reported for substituted aryl cations before [5b], the exothermicity of addition must be greater than the homolytic bond dissociation energies of the Ar–Br and $Ar–NO_2$ bonds (these are 80.5 and 71.3 kcal mol^{-1} for the neutral bromo and nitro benzene derivatives [26]). Related "charged phenyl radicals" have been synthesized (via CID on even electron precursor ions) and studied in the gas phase [27] and a search of the older chemical ionization mass spectrometry literature reveals that highly exothermic protonation of disubstituted benzene derivatives also yields related distonic ions [28]. Further studies aimed at providing evidence for distonic ions formation are discussed in Section 3.5.

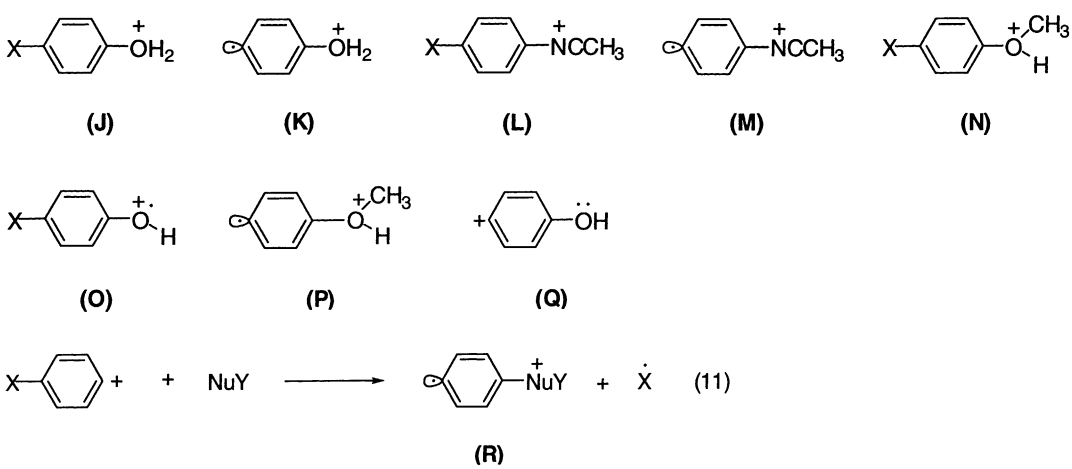

As noted previously, loss of N_2 in the gas phase is the principal dissociation pathway for the parent diazonium ions, resulting in highly reactive phenyl cations (Table 6). For the following reactions, only the most abundant product ions will be discussed and ions due to background reactions (with H_2O, CH_3OH and CH_3CN) will not be included.

Reaction of the aryl cations (*p*-$XC_6H_4^+$), with H_2O resulted in adduct formation for X = Cl, NO_2 and CH_3O (Eq. (5)), while for X = Br, adduct formation was followed by loss of Br to yield a distonic ion as the major product (Eq. (11)). To verify that these were oxygen protonated species, we performed CID on the adducts (Table 7). CID of protonated *p*-chlorophenol resulted in water loss, thereby regenerating the original aryl cation, while the other energized adducts also yielded fragmentation products consistent with oxygen protonation. These CID results will be explained in greater detail in Section 3.4.

Reaction of the substituted phenyl cations ($XC_6H_4^+$) with methanol (where X = Cl, Br, NO_2 and CH_3O), resulted in elimination of $CH_3^\bullet$ by cleavage of the O–C bond from the energized adduct X–$C_6H_5OH(CH_3)^+$ as the predominant pathway (Eq. (6)). In the case of X = CH_3O, deuterium labeling was employed to distinguish whether CH_3 loss was occurring from the *para* substituted CH_3O group or from addition of CH_3OH to the phenyl cation. In agreement with the above observations, loss of CH_3 was found to occur from the X–$C_6H_5OH(CH_3)^+$ species. Other workers [6,7b,8] have also observed this type of hydroxylation reaction in which the phenol molecular ion is formed, and have concluded it is the result of the phenyl cation reacting with the lone electron pair on oxygen to form *O*-protonated anisole.

Almost exclusive adduct formation was observed when the substituted phenyl cations were allowed to react with CH_3CN (Eq. (5)) as seen in Fig. 3. The MS/MS spectra of all four compounds clearly shows abundant adduct formation at *m/z* 152/154 (Fig. 3A), 196/198 (Fig. 3B), 163 (Fig. 3C) and 148 (Fig. 3D) for $XC_6H_4^+$ where X = Cl, Br, NO_2 and CH_3O, respectively. The most likely site of attack is the nitrogen lone pair of CH_3CN [29]. In addition to various other ion–molecule reactions with background gases, losses of NO (Eq. (12)) and NO_2 (cf. Eq. (11)) from the $O_2NC_6H_4NCCH_3^+$ adduct were also observed.

$$\underset{m/z\,122}{C_6H_4O_2N^+} + CH_3CN \rightarrow \underset{m/z\,133}{C_8H_7ON^{\bullet+}} + NO \qquad (12)$$

A different mode of reactivity was observed in ion–molecule reactions between the *para* substituted phenyl cations and $(CH_3)_2CO$, consistent with a previous study in which the phenyl cation was reacted with $(CH_3)_2CO$ to yield $C_7H_7O^+$ as the primary product [7b] (Eq. (13)). Although a mechanism was not given for this reaction, the product is derived from loss of C_2H_4 from the initial adduct. In our experiments, abundant adduct formation is observed when $XC_6H_4^+$ reacted with $(CH_3)_2CO$ (Eq. (5)) but the reaction paths of the decomposing adducts differed and were dependent upon the nature of the substituent. For example, when X = CH_3O the collisionally stabilized adduct was most prominent, followed by loss of C_2H_4 from the energized adduct (cf. Eq. (13)), while for X = Cl, the most abundant ion was due to loss of C_2H_4 from the adduct (cf. Eq. (13)). In contrast, when X = Br and NO_2, the most abundant product ions were due to Br and NO_2 loss from the adduct (which may lead to distonic ion formation cf. Eq. (11)). These results highlight the weaker bond strengths in Br–Ar and O_2N–Ar bonds [26]. Further investigation with $(CD_3)_2CO$ as the nucleophile yielded identical product ions with the appropriate mass shifts.

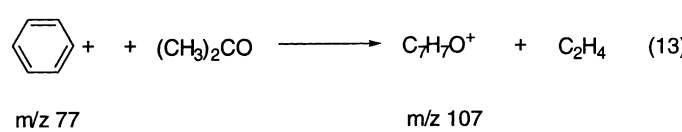

Reactions of aryl cations with peptide bonds have recently been investigated as a means of trapping peptides [1a]. Thus we were interested in examining the gas phase behavior of the substituted phenyl

Table 7
CID reactions of adducts of *para* substituted phenyl cations in the presence of nucleophiles

X	Nucleophile (Nu)	Products[a]
Cl	H_2O	B(100); J(17); K(32); O(79); 65(2); 93(66); 125(19); 134(23)
	CH_3OH	O(9); P(100); 72(15); 107(19); 124(6); 132(9)
	CD_3OD	D + Nu(9); D + 2Nu(11); O(8); 111(21); 112(30); 126(21); 129/131(9); 144(38); 146/148(100)
	CH_3CN	A(26); B(100); J(21); M(23); O(43); 125(19); 125 + Nu(8); 134(30)
	$(CH_3)_2CO$	$(Nu + H)^+$ (7); 141/143(100); 141/143 + Nu(15); 158/160(9)
	$(CD_3)_2CO$	$(Nu + H)^+$ (5); $(Nu + D)^+$ (2); 143/145(79); 144/146(100); 144/146 + Nu(21)
	$CH_3C(O)NHCH_2CH_3$	B(10); D + Nu(56); $(2Nu + H)^+$ (7); 70(100); 156/158(2); 156/158 + Nu(6)
	Pyrrole	$(Nu + H)^+$ (4); R(100)
	$C_6H_5NH_2$	D + Nu(6); $(Nu + H)^+$ (23); $Nu^{\bullet +}$ (8); R(100)
Br	H_2O	K(100)
	CH_3OH	D + Nu(17); P(100); 138(6); 157/159(49); 176/178(15); 179(15); 191(42); 191 + Nu(6); 200(11); 210(4)
	CD_3OD	110(49); 111(36); 112(100); 113(15); 159(9); 173/175(5); 191/193 + Nu(34); 196/198 + Nu(17); 201(11)
	CH_3CN	A(11); B(15); D + Nu(7); J(10); K(25); M(17); O(22); P(6)
	$(CH_3)_2CO$	R(100); R + Nu(10); 141(8); 185/187(11); 185/187 + Nu(4)
	$(CD_3)_2CO$	R(100); R + Nu(9); 188/190(8); 188/190 + Nu(2)
	$CH_3C(O)NHCH_2CH_3$	D + Nu(100); $(2Nu + H)^+$ (1); R(1); 70(27); 121(1); 200/202(2); 200/202 + Nu(6)
	Pyrrole	$(Nu + H)^+$ (4); R(100)
	$C_6H_5NH_2$	D + Nu(4); $(Nu + H)^+$ (23); $Nu^{\bullet +}$ (9); R(100); 199(1); 199 + Nu(13); 230(2); 230 + Nu(2); 265(6); 265 + Nu(11)
NO_2	H_2O	K(49); 109(5); 123(100)
	CH_3OH	P(8); 137(100)
	CD_3OD	112(6); 140(100)
	CH_3CN	M(100); 133(42)
	$(CH_3)_2CO$	D + Nu(6); R(100); R + Nu(8); 163(11)
	$(CD_3)_2CO$	R(100); R + Nu(8); 138(25); 169(6)
	$CH_3C(O)NHCH_2CH_3$	D + Nu(100); $(Nu + H)^+$ (1); $(2Nu + H)^+$ (4); R(7); R + Nu(11); 70(74); 121(2)
	Pyrrole	B(8); D + Nu(75); $(Nu + H)^+$ (3); R(100); R + Nu(34); 116(6); 131(68); 151(4);157(26);159(19);172(6);183(13)
	$C_6H_5NH_2$	D + Nu(19); $(Nu + H)^+$ (19); R(21); 198(100); 230(4); 230 + Nu(9)
OCH_3	H_2O	65(5); 93(100); 110(58); 111(99); 134(22)
	CH_3OH	B(32); O(100); 109(9); 128(6)
	CD_3OD	D + Nu(21); 101(15); 110(36); 110 + Nu(13); 125(100); 128(96)
	CH_3CN	B(6); N(6); 118(100); 125(60); 133(10); 135(13)
	$(CH_3)_2CO$	J(13); 133(25); 137(100); 137 + Nu(6)
	$(CD_3)_2CO$	138(11); 139(85); 140(100); 140 + Nu(8); 141(47); 142(9); 143(32)
	$CH_3C(O)NHCH_2CH_3$	B(1); D + Nu(25); $(2Nu + H)^+$ (2); 70(100); 152(2); 152 + Nu(6)
	Pyrrole	B(2); $(Nu + H)^+$ (2); R(13); R + Nu(19); 159(100)
	$C_6H_5NH_2$	B(4); D + Nu(2); $(Nu + H)^+$ (100); 123(27); 168(96); 168 + Nu(4); 169(36); 185(88); 215(10)

[a] Only products with 1% or greater relative abundance are listed.

cations with a model system, *N*-ethylacetamide. For *p*-$XC_6H_4(Nu)^+$ where X = Cl, Br and NO_2, the most dominant peak in the spectra was $(Nu + H + Nu)^+$, while for X = CH_3O direct adduct formation was most abundant (Eq. (5)). Due to the presence of two nucleophilic sites (i.e., nitrogen and oxygen) we were interested in determining the regioselectivity of these arylation reactions. Under these experimental conditions, *O*-arylation seems to be favored over *N*-arylation due to the presence of an abundant fragmentation product ion $(CH_2CH_3NCCH_3)^+$ at *m*/*z* 70 (Eq. (14)) in all four cases. There were, however,

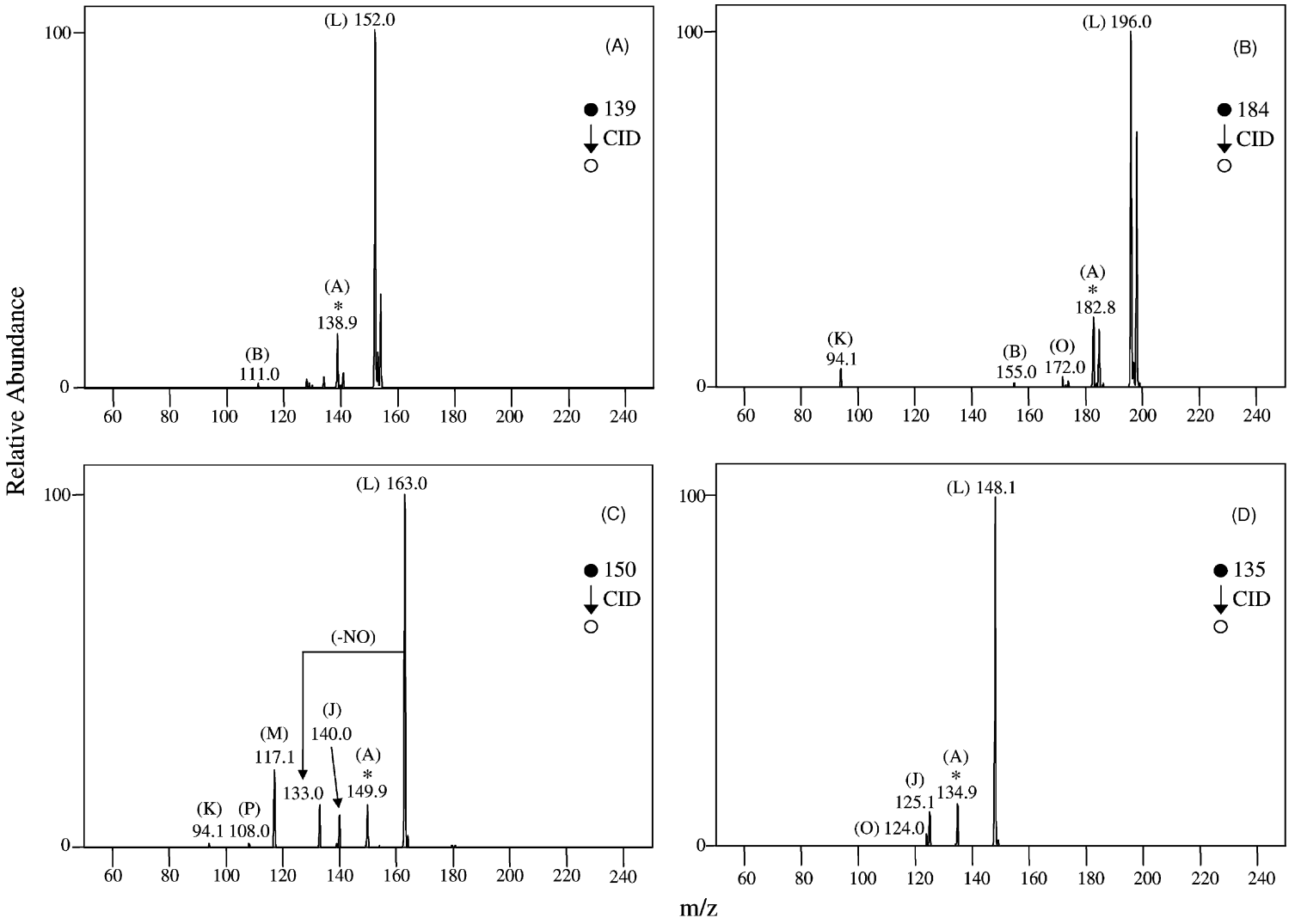

Fig. 3. CID MS^2 of p-X–$C_6H_4N_2^+$ in the presence of acetonitrile, where X = (A) Cl, (B) Br, (C) NO_2 and (D) OCH_3.

minor product ions due to *N*-arylation (loss of CH_2CO from the adduct) (Eq. (15)).

The thermodynamic preference for *O*-alkylation over *N*-alkylation has been noted from ab initio calculations on $HC(O)NH_2$ [30]. Furthermore, experiments in both the condensed phase [1a,31a] and the gas phase [31b] support a kinetic preference for *O*-alkylation. CID experiments on the adducts are discussed in greater detail in Section 3.4. The appearance of the $(Nu + H)^+$ and $(Nu + H + Nu)^+$ product ions were attributed to proton transfer reaction pathways resulting in benzyne formation (cf. Eq. (8)).

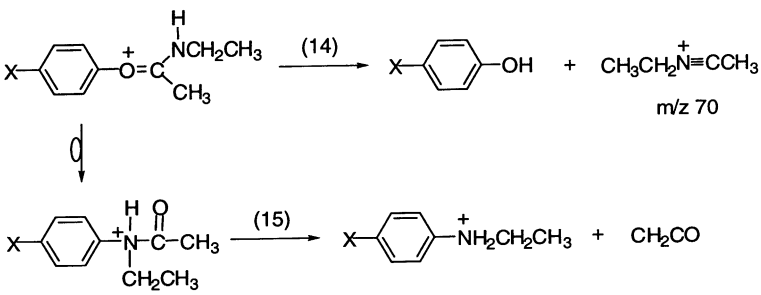

The gas phase behavior of the substituted phenyl cations ions towards pyrrole were also examined. For *p*-$XC_6H_4N_2^+$ where X = MeO, adduct formation was observed as the most abundant product ion (Eq. (5)), while for X = Cl, Br and NO_2, initial adduct formation was followed by loss of the substituents, presumably yielding distonic ions (Eq. (11)). In addition to adduct formation, proton transfer to pyrrole (and subsequent benzyne formation) was a feature in all of the spectra, while electron transfer from the nucleophile was more prominent, particularly when X = NO_2. The observation of electron transfer may support previously proposed mechanisms for adduct formation in heteroarenes, in which single-electron transfer (SET) from the heteroarene to the electrophile is followed by recombination of the of the radicals to yield a sigma bonded intermediate (Eq. (16)) [32].

The final neutral reagent studied was aniline. In the case of the electron withdrawing substituents (i.e., Cl, Br, NO_2) electron transfer dominated the spectra, in addition to relatively abundant distonic ions (Eq. (11)). Proton transfer to aniline also occurred but was minor in comparison. For the electron donating CH_3O substituent, formation of the adduct was the main feature of the spectrum with relatively minor product ion contributions from both electron and proton transfer.

3.4. CID reactions of adducts of para substituted phenyl cations, p-XC_6H_4-Nu^+ (where X = Cl, Br, NO_2,OCH_3)

To further investigate the reaction pathways described in Section 3.3, CID experiments were performed on the adducts *p*-XC_6H_4-Nu^+. These adducts were formed via ion–molecule reactions between non-mass selected aryl cations formed via in source CID on their diazonium precursor ions and the neutral nucleophiles during the ion accumulation period (typically 100 ms). The results of these experiments are listed in Table 7and shown in Figs. 4 and 5.

Collisional activation of the stable *p*-$XC_6H_4OH_2^+$ adducts resulted in either H_2O or X loss. When X = Cl, regeneration of the phenyl cation was observed as the primary fragmentation pathway (i.e., the reverse of Eq. (5)), closely followed by Cl loss. In the cases where X = Br and NO_2, loss of X was also seen. Loss of HO from the *p*-$O_2NC_6H_4OH_2^+$ adduct was also

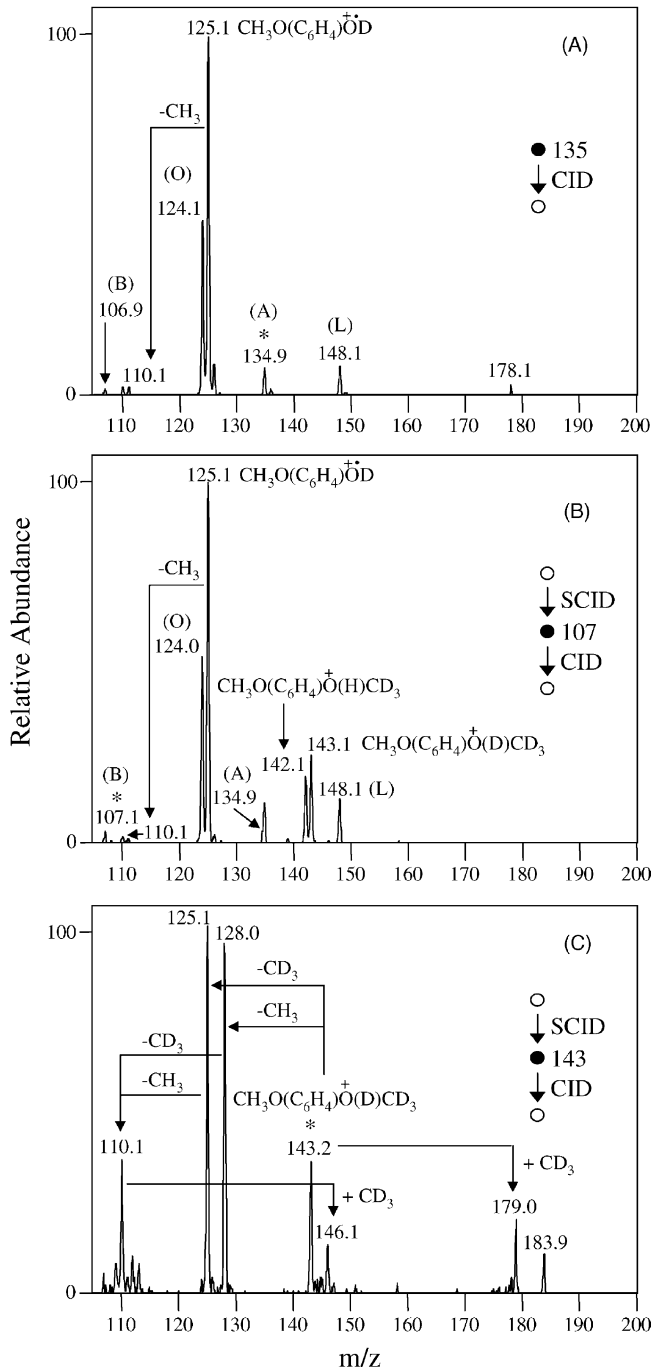

Fig. 4. (A) CID MS^2 of *p*-CH_3O–$C_6H_4N_2^+$ in the presence of CD_3OD, (B) ion–molecule reactions of source generated *p*-CH_3O–$C_6H_4^+$ with CD_3OD, (C) CID of the collisionally stabilized [*p*-CH_3O–$C_6H_4OCD_3$ + D]$^+$ adduct ion.

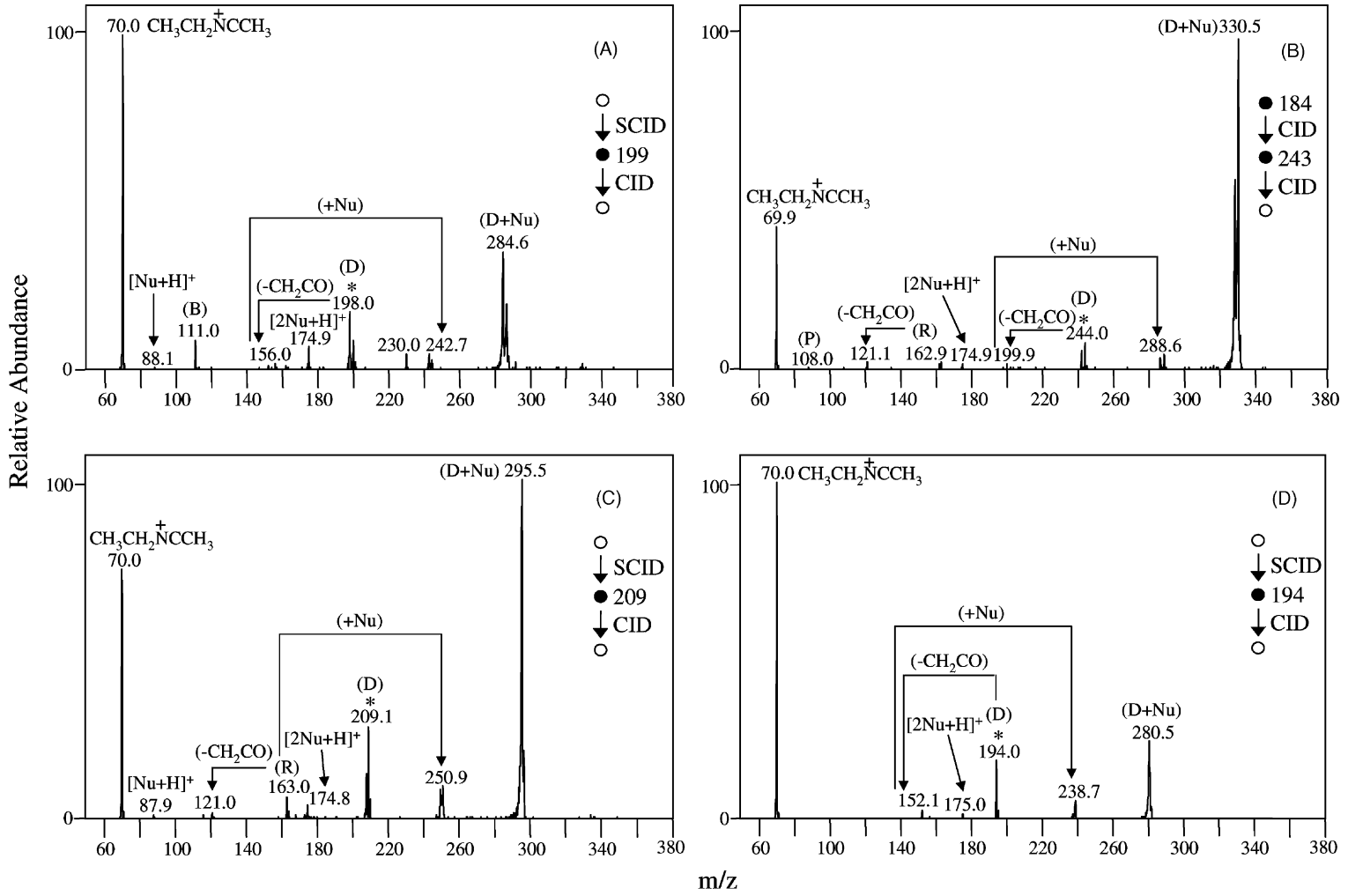

Fig. 5. CID MS^2 of *p*-X–$C_6H_4(CH_3CONHCH_2CH_3)$ where X = (A) Cl, (B) Br, (C) NO_2 and (D) OCH_3.

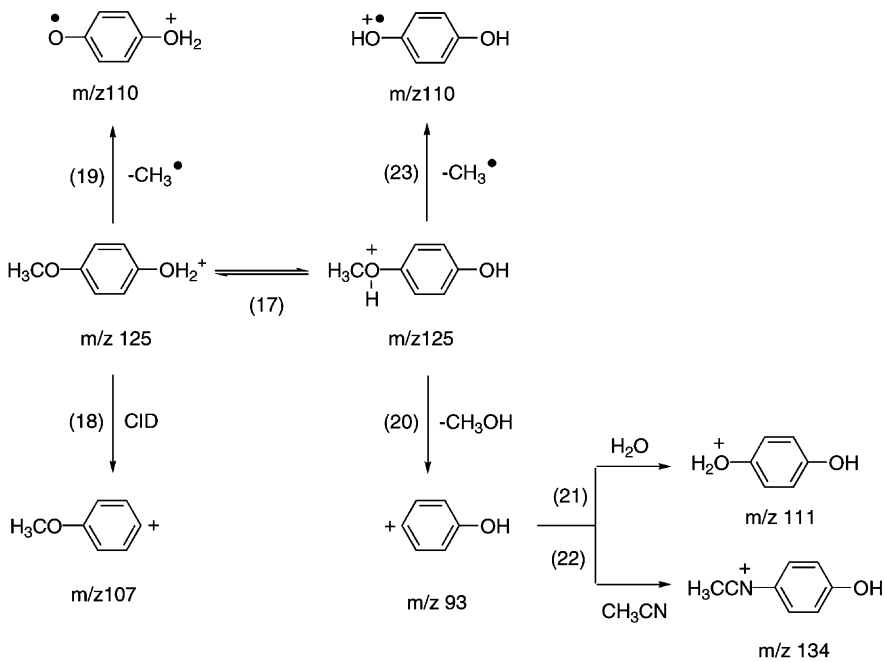

Scheme 1.

observed. The exact mechanisms for all of these reactions are uncertain. While it is tempting to speculate that loss of X results in the formation of distonic ions (cf. Eq. (11)), the formation of other isomers such as the conventional radical cations of phenols is possible.

A number of interesting dissociation product ions were observed when X = CH_3O. Scheme 1 shows the initial adduct can be subject to proton transport where either the *para* substituent or the attached nucleophile may be protonated (Eq. (17)) [13]. Upon CID of *p*-$H_3COC_6H_4OH_2^+$ two possible fragmentation pathways exist i.e., regeneration of the phenyl cation (Eq. (18)) or loss of $CH_3^\bullet$ to give a product ion at *m*/*z* 110 (Eq. (19)). Our experimental data suggests the reaction most likely occurs when the proton resides on the methoxy substituent as abundant ions are seen at *m*/*z* 93, 111, 134 and 110, respectively (Eq. 20–23). Loss of CO from the product ion at *m*/*z* 93 was also observed and can be attributed to ring protonation, which accounts for a small fraction of the protonated phenol ions. (The mechanism for CO loss from the radical cation of phenol has been discussed—see [33].)

The stabilized *p*-$XC_6H_4OH(CH_3)^+$ adducts arising from reactions between methanol and the aryl cations were also subjected to CID. When X = Cl and Br loss of X was the primary fragmentation pathway (cf. Eq. (11)), while for X = NO_2, OH loss yielded the most predominant ion. Once again, the precise mechanisms of these reactions are uncertain. As CH_3–O bond homolysis was observed to occur almost exclusively for X = CH_3O, CD_3OD was employed to ascertain whether CH_3 loss was occurring from the *para* substituent or from the addition of methanol to the phenyl cation (Fig. 4 and Scheme 2).

The issue of isomerization of adduct ions can be addressed by comparing the fragmentation reactions of the energized adducts with their long lived collisionally stabilized adduct. Thus, the energized adducts formed in the reactions of CD_3OD with CID generated aryl cations (Fig. 4A) fragment via loss of $CD_3^\bullet$ as do the adducts formed from mass selected aryl cations (Fig. 4B). In contrast, the long lived *p*-$CH_3OC_6H_4OD(CD_3)^+$ adduct ion fragments via loss of both $CD_3^\bullet$ and $CH_3^\bullet$ (Fig. 4C).

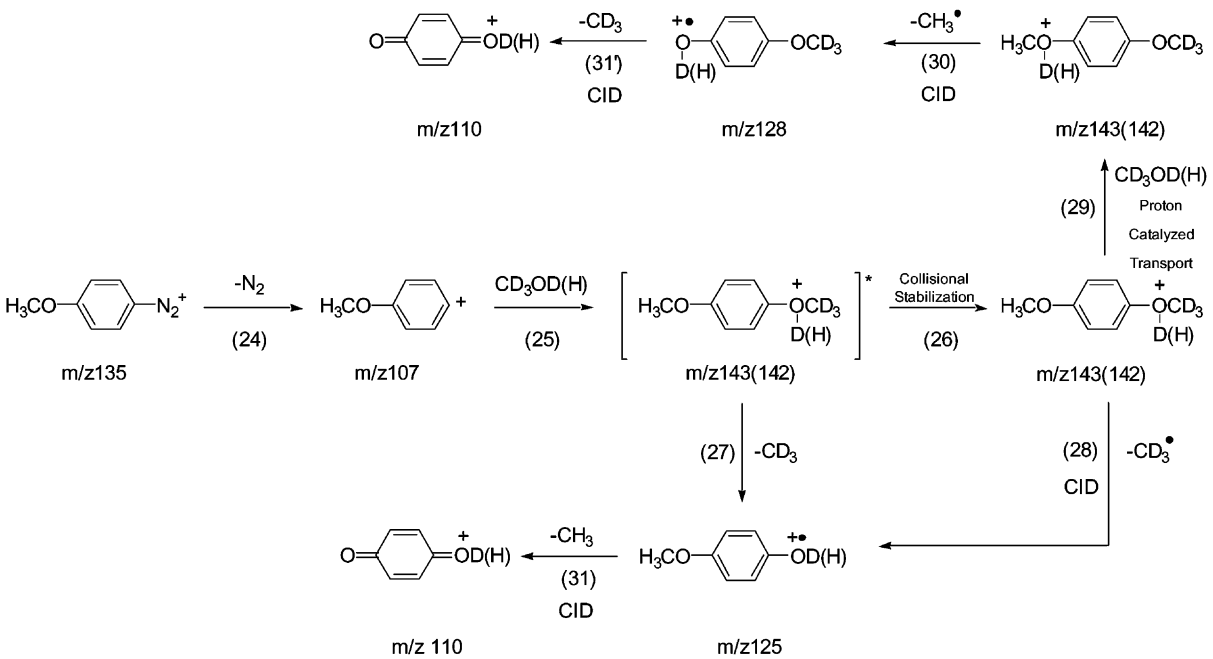

Scheme 2.

These observations can be rationalized by examining Scheme 2. Upon initial dediazoniation (Eq. (24)), the phenyl cation can readily react with $CD_3OD(H)$ (Eq. (25)) resulting in an energized adduct (Eq. (26)), which can either undergo collisional stabilization (Eq. (26)) or fragmentation via exclusive loss of $CD_3^\bullet$ (Eq. (27)). Subsequent $CH_3^\bullet$ loss from the ion at *m/z* 125 also occurs but to a minor extent (Eq. (31)). CID of the collisionally stabilized adduct (Fig. 4C) however, reveals two processes: (a) loss of $CD_3^\bullet$ (Eq. (28)) and (b) $CH_3^\bullet$ loss (Eq. (30)). The most likely explanation of these competitive losses is that there are two populations of adduct ions, $CH_3OC_6H_4O(D)CD_3^+$ and $CH_3O(D)C_6H_4OCD_3^+$, which can interconvert via proton catalyzed transfer (Eq. 29). Subsequent losses of $CD_3^\bullet$ (Eq. (31′) and $CH_3^\bullet$ (Eq. (31)) are both responsible for the product ion at *m/z* 110.

The stable *p*-$XC_6H_4NCCH_3^+$ adducts were also subjected to CID. When X = Cl, the *para* substituted phenyl cation was regenerated, while for X = Br, the distonic ion (Eq. (11)) and phenyl cation were in relatively equal abundances. When X = NO_2, NO loss (Eq. (12)) in addition to distonic ion formation were observed, while for X = CH_3O, distonic ion formation was most prominent (Eq. (11)). Further studies aimed at providing evidence for the formation of distonic ions when X = NO_2 are discussed in Section 3.5.

The manner in which the collisionally stabilized *p*-$XC_6H_4OC(CH_3)_2^+$ adducts fragmented was quite interesting. In the case of X = Cl and CH_3O, C_2H_4 loss was followed by loss of 28, while for X = Br and NO_2, distonic ion formation was followed by the stepwise loss of $CH_3^\bullet$ and 28. To determine whether CO or C_2H_4 loss was occurring, $OC(CD_3)_2$ was used to generate the *p*-$XC_6H_4OC(CD_3)_2^+$ adducts. CID of these adducts showed C_2D_3H loss followed by loss of 28 for X = Cl and CH_3O (Eq. (32)), while for X = Br and NO_2, distonic ion formation was followed by CD_3 and 28 loss (Eq. (33)). Thus, from these observations it was clear that CO loss (from the ring) was occurring. Due to the presence of H-D scrambling it was difficult to ascertain the exact mechanism(s) for

each of these reactions.

$$(\text{X-C}_6\text{H}_4\text{OC(CD}_3)_2)^+ \overset{-\text{C}_2\text{D}_3\text{H}}{\underset{\text{CID}}{\rightarrow}} (\text{X-C}_7\text{H}_3\text{D}_3\text{O})^+ \quad (\text{X=Cl, CH}_3\text{O})$$

$$\overset{-\text{CO}}{\underset{\text{CID}}{\rightarrow}} (\text{X-C}_6\text{H}_3\text{D}_3)^+ \qquad (32)$$

$$(\text{X-C}_6\text{H}_4\text{OC(CD}_3)_2)^+ \overset{-\text{X}}{\underset{\text{CID}}{\rightarrow}} (\text{C}_6\text{H}_4\text{OC(CD}_3)_2)^{\bullet+} \quad (\text{X=Br, NO}_2)$$

$$\overset{-\text{CD}_3}{\underset{\text{CID}}{\rightarrow}} (\text{C}_8\text{H}_4\text{D}_3\text{O})^{\bullet+} \overset{-\text{CO}}{\underset{\text{CID}}{\rightarrow}} (\text{C}_7\text{H}_4\text{D}_3)^{\bullet+} \qquad (33)$$

In order to gain a better understanding of the fragmentation behavior of the *p*-$XC_6H_4OHC(CH_3)N(CH_3CH_2)^+$ adducts, they were subjected to CID (Fig. 5). Upon examination of Fig. 5, *O*-arylation was clearly preferred with the product ion $(CH_3CH_2NCCH_3)^+$ (*m/z* 70) (Eq. 4)) dominating. Minor fragments due to *N*-arylation were also present in all spectra (Eq. (15)). To further investigate the appearance of both *N*- and *O*-arylation product ions, and to determine whether these adducts can isomerize, *p*-Br-*N*-ethyl-acetanilide (*p*-$BrC_6H_4N(CH_2CH_3)(COCH_3)$) was independently synthesized and the fragmentation behavior of its $[M + H]^+$ ion was examined by CID. The resultant spectrum is shown in Fig. 6 and can be compared to the adduct formed via ion–molecule reactions (Fig. 5B). The base peak at *m/z* 200 and 202 is consistent with decomposition of the *N*-protonated ion via CH_2CO loss (Eq. (34)). The very small peak at *m/z* 70 (1% abundance), suggests that the *N*-protonated ion undergoes isomerization (Eq. (35)) followed by fragmentation (Eq. (36)). (The radical cations of amides undergo a similar rearrangement see [34].) Several other product ions were also observed including Br loss (*m/z* 163) followed by loss of CH_2CH_3 (*m/z* 135) and the combined losses of Br and CH_2CO (*m/z* 121).

Loss of X was the major fragmentation pathway for $XC_6H_4(\text{pyrrole})^+$ where X = Cl, Br and NO_2, while X = CH_3O fragmented via CH_3 loss. There was also some minor product ions due to the formation of protonated pyrrole, which are likely to arise from proton transfer and subsequent benzyne formation.

CID of $XC_6H_4(\text{aniline})^+$ for X = Cl and Br gave abundant loss of X, while this was a minor channel for X = NO_2 where OH loss dominated instead. The fragmentation pattern of the adduct where X = CH_3O was slightly more complicated and was dominated by the formation of protonated aniline. For the adducts derived from X = Cl, Br and NO_2, proton transfer to aniline was also observed in addition to some electron transfer.

3.5. Probing regioselectivity in N_2 loss from isomeric diazonium ions and distonic ion formation

In order to examine the issues of isomerization of $XC_6H_4^+$ aryl cations and their $XC_6H_4NuY^+$ adduct ions, the *ortho* and *meta* derivatives of $O_2NC_6H_4N_2BF_4^-$ were synthesized, and the fragmentation reactions of their free diazonium ions were compared to the *para* isomer. We were particularly

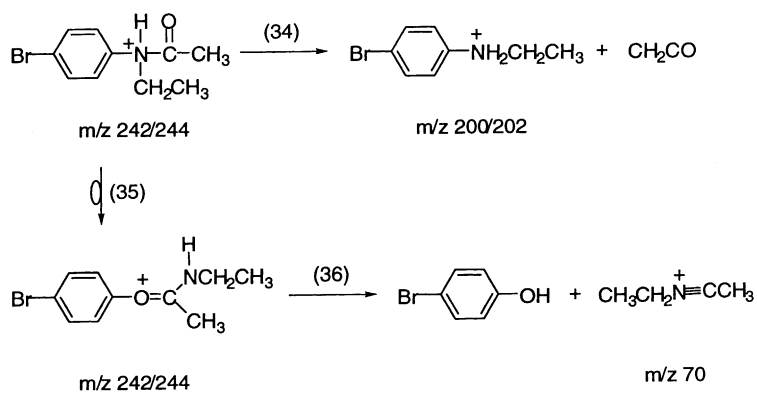

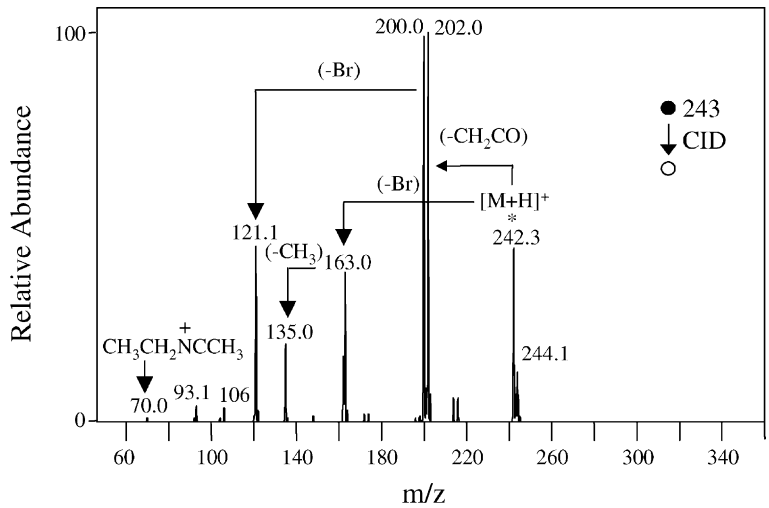

Fig. 6. CID MS^2 of *p*-Br–$C_6H_4NH(C(O)CH_3)(CH_2CH_3)^+$.

interested in using ion–molecule reactions with allyl iodide to address whether true distonic ions were formed. This requires the adducts to be synthesized in a separate step, and so we decided to form these via in source CID from solutions of the appropriate diazonium ion in either pure acetonitrile or methanol. This approach also gave us an opportunity to examine CID of the diazonium ions in the ion trap in the absence of a mixture of ESI solvent gases.

When CID of the diazonium ions generated from ESI of their salts in pure acetonitrile were carried out in the ion trap, the spectra shown in Fig. 7 resulted. The major difference between the CID of the *para* isomer under these conditions (Fig. 7C) and when acetonitrile was added to the bath gas (Fig. 3C) is that the arylcation is formed in much higher abundance to its ion–molecule reaction products. Nonetheless, products due to ion–molecule reactions with background gases (mainly water and acetonitrile) are still observed. An examination of Fig. 7 reveals that there are significant differences between the CID spectra of the *ortho* isomer relative to the *meta* and *para* isomers. Perhaps the most dramatic difference is that the aryl cations are the base peak in the CID spectra of the *meta* and *para* isomers (Fig. 7B and C) but are virtually non-existent in the *ortho* isomer (Fig. 7A). The only difference between the CID spectra of the *meta* and *para* diazonium was due to minor product ions (1%, relative to base peak) at *m*/*z* 110 for *m*-$O_2NC_6H_4N_2^+$ and at *m*/*z* 79 and 117 for *p*-$O_2NC_6H_4N_2^+$.

Given that aryl cations and their adducts with acetonitrile were only observed for the *meta* and *para* isomers, we next studied the CID of source generated *meta* and *para* $O_2NC_6H_4NCCH_3^+$ adduct ions. The resultant spectra are given in Fig. 8 and show that both isomers fragment via abundant NO_2 loss. The only subtle difference between the two spectra is that the *para* isomer gives a minor ion at *m*/*z* 105 (Fig. 8A) which is absent for the *meta* isomer, while the *meta* isomer in turn gives an unique minor ion at *m*/*z* 92 (Fig. 8B). To provide evidence that the ions due to NO_2 loss are distonic ions, they were mass selected and allowed to react with allyl iodide [27]. Fig. 9 shows that the ions at *m*/*z* 117 originating from the *para* (Fig. 9A) and *meta* (Fig. 9B) diazonium ions both react via iodine abstraction as the main reaction pathway (*m*/*z* 244), with a small amount of allyl radical transfer present (*m*/*z* 158). These results suggest that these ions do have a distonic ion structure.

The same types of experiments were repeated with ESI solutions of the diazonium salts in pure methanol. Once again, there was a dramatic difference in the CID

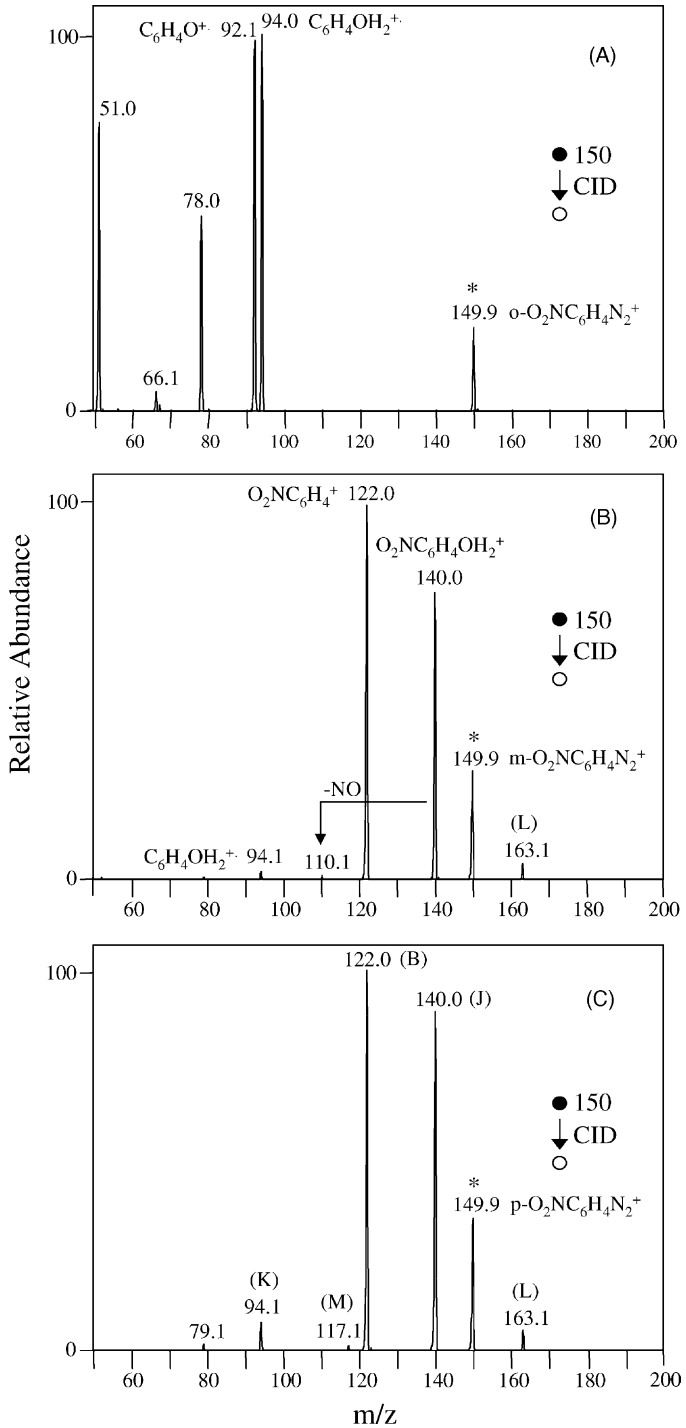

Fig. 7. CID MS^2 of isomers of nitrobenzenediazonium ions dissolved in pure CH_3CN: (A) *o*-O_2N–$C_6H_4N_2^+$, (B) *m*-O_2N–$C_6H_4N_2^+$, (C) *p*-NO_2–$C_6H_4N_2^+$.

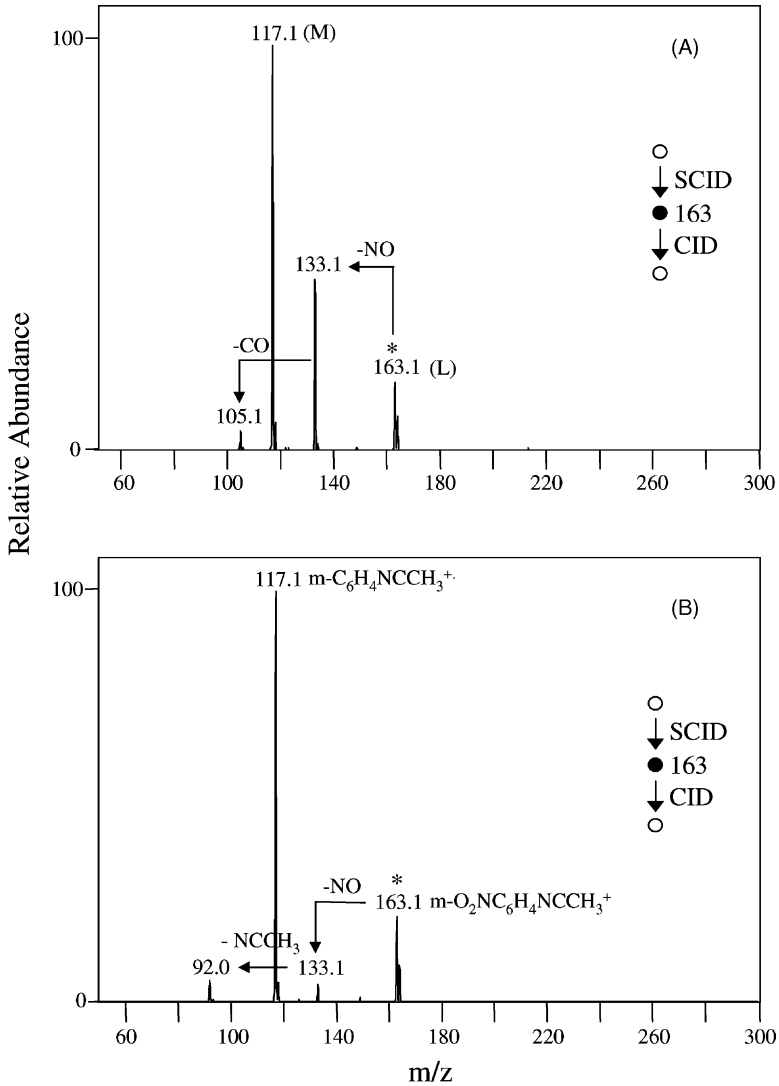

Fig. 8. CID MS^2 of source formed adduct ions: (A) *p*-O_2N–$C_6H_4NCCH_3^+$ and (B) *m*-O_2N–$C_6H_4NCCH_3^+$.

spectra of *o*-$O_2NC_6H_4N_2^+$ (Fig. 10A) relative to the *meta* (Fig. 10B) and *para* (Fig. 10C) isomers. Interestingly, the CID spectra for the *ortho* isomer formed from the methanol ESI solvent (Fig. 10A) is similar to that obtained when acetonitrile is used as the solvent (Fig. 7A). In contrast the abundances of the aryl cations observed in the CID spectra of the *meta* and *para* isomers formed from the methanol ESI solvent (Fig. 10B and C) are significantly diminished to those obtained when acetonitrile was used as the solvent (Fig. 7B and C). The spectra for the *meta* and *para* isomers are very similar, with a water adduct (*m*/*z* 140) being the most abundant ion in both cases. Only subtle differences between the *meta* and *para* isomers are observed in their formation of minor ions at *m*/*z* 79, 110, 122 and 123.

The CID of the source formed adduct ions were also examined (data not shown). For *m*-$O_2NC_6H_4$ $(CH_3OH)^+$, we observed loss of NO_2 (*m*/*z* 108) as the sole fragment ion, while for *p*-$O_2NC_6H_4$ $(CH_3OH)^+$,

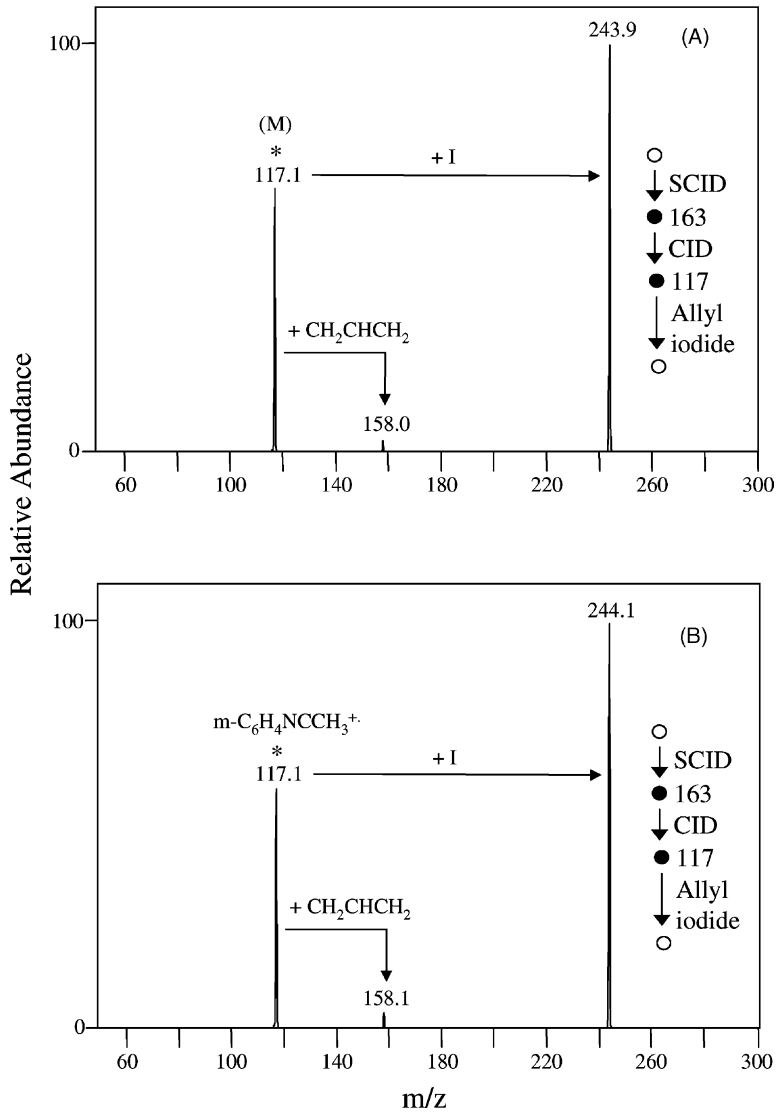

Fig. 9. Ion–molecule reactions of the mass selected distonic ions with allyl iodide: (A) distonic ion formed from *p*-O_2N–$C_6H_4NCCH_3^+$ and (B) distonic ion formed from *m*-O_2N–$C_6H_4NCCH_3^+$.

OH loss (*m*/*z* 137) gave the base peak (100%) along with product ions at *m*/*z* 108 (51%) and 113 (8%). In an attempt to determine whether the observed losses of NO_2 yielded the distonic ions for the *meta* and *para* systems, ion–molecule reactions with allyl iodide were once again employed (data not shown). In contrast to the distonic ion derived from acetonitrile (Fig. 9), both product ions at *m*/*z* 108 did not readily react with the allyl iodide, with ions corresponding to iodine abstraction (*m*/*z* 235) and allyl radical transfer (*m*/*z* 149) present in only trace amounts (~1%). One possibility for this dramatic difference is that the methoxy distonic ions are inherently less reactive. An alternative explanation is that they rearrange via intramolecular or bimolecular catalyzed H transfer to the conventional radical cations of anisole.

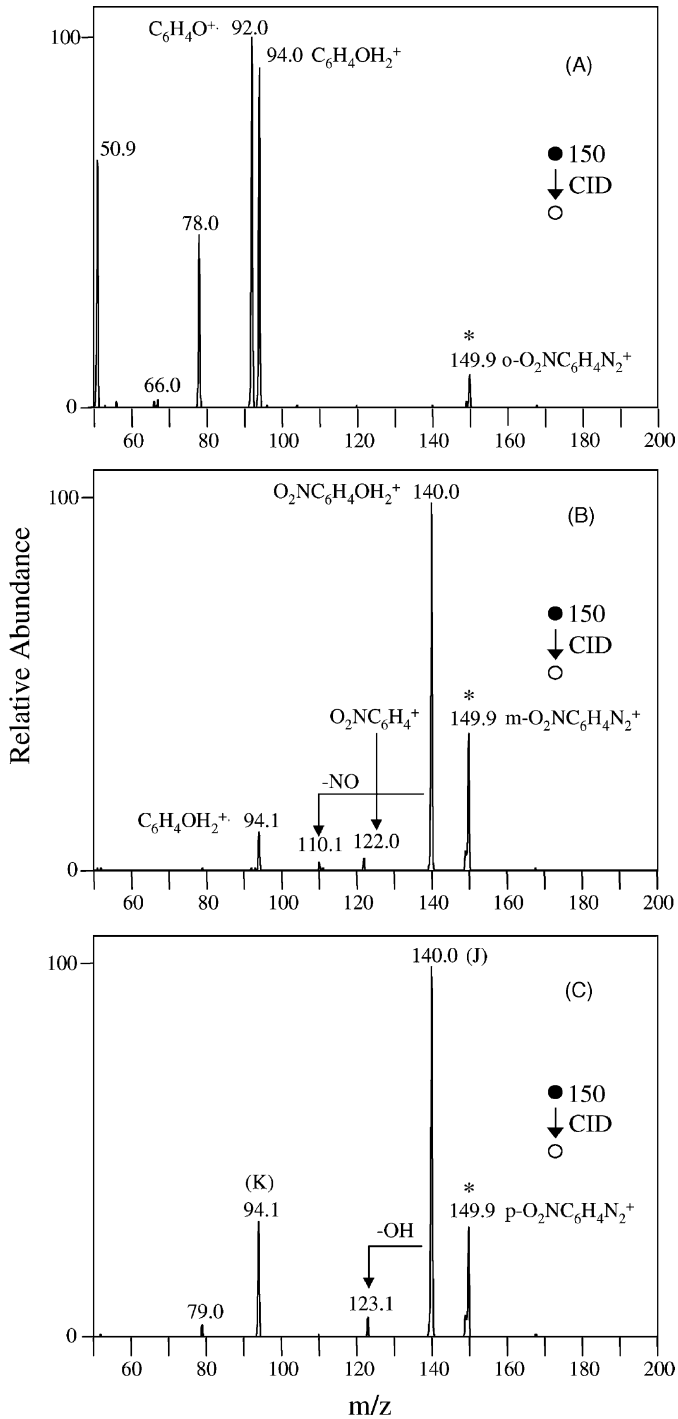

Fig. 10. CID MS^2 of isomers of nitrobenzenediazonium ions dissolved in pure CH_3OH: (A) *o*-O_2N–$C_6H_4N_2^+$, (B) *m*-O_2N–$C_6H_4N_2^+$, (C) *p*-NO_2–$C_6H_4N_2^+$.

4. Conclusions

Electrospray ionization of the tetrafluoroborate salts of *para* substituted (chloro, bromo, nitro and methoxy) benzene diazonium ions ($XC_6H_4N_2^+$ where X = Cl, Br, NO_2 and CH_3O) results in the formation of the bare diazonium ion as well as the mixed inorganic/organic salt ion clusters in both the positive and negative mode. Evidence of "magic numbers" were observed in the case of $(p\text{-}XC_6H_4N_2^+BF_4^-)_nXC_6H_4N_2^+$ and $(p\text{-}XC_6H_4N_2^+BF_4^-)_nBF_4^-$ where X = Cl, Br and NO_2 in which the key cluster ions were at $n = 1$ and 4, while for X = CH_3O, the most abundant cluster ions were at $n = 1$ and 6. The diazonium ions were generally found to be unreactive towards the nucleophiles, while the opposite trend emerged for the substituted phenyl cations. These were found to readily form energized adducts ($XC_6H_4NuY^+$), which underwent several different fragmentation reactions, including radical loss of the *para* substituent. The gas phase CID reactions of the adducts ($XC_6H_4NuY^+$) were also examined, and similar types of reactions were observed. Ion–molecule reactions with allyl iodide provided evidence for distonic ion formation via loss of NO_2 from the *meta* and *para* aryl cation adducts $O_2NC_6H_4NCCH_3^+$.

Acknowledgements

A.K.V. acknowledges the financial support of a Science Faculty Scholarship (Students). R.A.J.O. thanks the Australian Research Council for financial support and the University of Melbourne for funds to purchase the LCQ. We thank I. Vrionis and N.K. Androutsopoulos for carrying out some preliminary experiments and both reviewers for useful comments.

References

[1] (a) L.S. Romsted, J. Zhang, L. Zhuang, J. Am. Chem. Soc. 120 (1998) 10046;
(b) H. Zollinger, Diazo Chemistry I, VCH, Weinheim, 1994;
(c) H. Mayr, M. Hartnagel, K. Grimm, Lieb. Ann. 1 (1997) 55;
(d) J.F. Brunnett, C. Yijima, J. Org. Chem. 42 (1977) 639.
[2] Heats of formation are from NIST Standard Reference Database Number 69—July 2001 Release, http://webbook.nist.gov/chemistry
[3] (a) R. Glaser, C.J. Horan, J. Org. Chem. 60 (1995) 7518;
(b) R. Glaser, C.J. Horan, H. Zollinger, Angew Chem. Int. Ed. Engl. 36 (1997) 2210.
[4] (a) M.S. Foster, J.L. Beauchamp, J. Am. Chem. Soc. 94 (1972) 2425;
(b) M.S. Foster, A.D. Williamson, J.L. Beauchamp, Int. J. Mass Spectrom. Ion Phys. 15 (1974) 429;
(c) P. Natalis, J.L. Franklin, Int. J. Mass Spectrom. Ion Phys. 40 (1981) 35;
(d) F. Cacace, F. Grandinetti, F. Pepi, J. Chem. Soc. Chem. Commun. 18 (1994) 2173;
(e) T.J. Broxton, R. Colton, J.C. Traeger, J. Mass Spectrom. 30 (1995) 319;
(f) T.J. Broxton, R. Colton, J.C. Traeger, J. Phys. Org. Chem. 8 (1995) 351.
[5] (a) M. Speranza, Chem. Rev. 93 (1993) 2933;
(b) A. Filippi, G. Lilla, G. Occhiucci, C. Sparapani, O. Ursini, M. Speranza, J. Org. Chem. 60 (1995) 1250, and references cited therein;
(c) G. Angelini, S. Fornarini, M. Speranza, J. Am. Chem. Soc. 104 (1982) 4773.
[6] G.G. Dolnikowski, J. Allison, J.T. Watson, Org. Mass Spectrom. 25 (1990) 119.
[7] (a) M. Speranza, M.D. Sefcik, J.M.S. Henis, P.P. Gaspar, J. Am. Chem. Soc. 99 (1977) 5583;
(b) P. Ausloos, S.G. Lias, T.J. Buckley, E.E. Rogers, Int. J. Mass Spectrom. Ion Proc. 92 (1989) 65.
[8] Y.A. Ranasinghe, G.L. Glish, J. Am. Soc. Mass Spectrom. 7 (1996) 473.
[9] (a) E.M. Evleth, P.M. Horowitz, J. Am. Chem. Soc. 93 (1971) 5636;
(b) H.H. Jaffe, G.F. Koser, J. Org. Chem. 40 (1975) 3082;
(c) C.G. Swain, J.E. Sheats, D.G. Gorenstein, K.G. Harbison, J. Am. Chem. Soc. 97 (1975) 791;
(d) J.D. Dill, P.V.R. Schleyer, J.S. Binkley, R. Seeger, J.A. Pople, E. Haselbach, J. Am. Chem. Soc. 98 (1976) 5428;
(e) A. Nicolaides, D.M. Smith, F. Jensen, L. Radom, J. Am. Chem. Soc. 119 (1997) 8083;
(f) M. Tasaka, M. Ogata, H. Ichikawa, J. Am. Chem. Soc. 103 (1981) 1885.
[10] E.D. Nelson, H.I. Kenttamaa, J. Am. Soc. Mass Spectrom. 12 (2001) 258.
[11] D. Schroder, K. Schroeter, W. Zummack, H. Schwarz, J. Am. Soc. Mass Spectrom. 10 (1999) 878.
[12] I.S. Ignatyev, T. Sundius, Chem. Phys. Lett. 326 (2000) 101.
[13] D.K. Bohme, Int. J. Mass Spectrom. Ion Proc. 115 (1992) 95.
[14] I.S. Ignatyev, T. Sundius, J. Phys. Chem. A 105 (2001) 4535.
[15] (a) O. Tishchenko, N.-N. Pham-Tran, E.S. Kryachko, M.T. Nguyen, J. Phys. Chem. A 105 (2001) 8709;
(b) N. Solca, O. Dopfer, Chem. Phys. Lett. 342 (2001) 191;
(c) M. Eckert-Maksic, M. Klessinger, Z.B. Maksic, Chem. Phys. Lett. 232 (1995) 472;
(d) K.V. Wood, D.J. Burinsky, D. Cameron, R.G. Cooks, J. Org. Chem. 48 (1983) 5236;

(e) J. Catalan, M. Yanez, J. Chem. Soc. Perkin Trans. 2 (1979) 741;
(f) D.J. DeFrees, R.T. McIver Jr., W.J. Hehre, J. Am. Chem. Soc. 99 (1977) 3853;
(g) D.P. Martinsen, S.E. Buttrill Jr., Org. Mass Spectrom. 11 (1976) 762;
(h) Y.K. Lau, P. Kebarle, J. Am. Chem. Soc. 98 (1976) 7452.
[16] H.T. Le, R. Flammang, P. Gerbaux, G. Bouchoux, M.T. Nguyen, J. Phys. Chem. A 105 (2001) 11582.
[17] (a) H.E. Audier, T.H. Morton, Int. J. Mass Spectrom. 185–187 (1999) 393;
(b) A.G. Harrison, Y.-P. Tu, Int. J. Mass Spectrom. 195/196 (2000) 33.
[18] G.E. Reid, R.A.J. O'Hair, M.L. Styles, W.D. McFadyen, R.J. Simpson, Rapid Commun. Mass Spectrom. 12 (1998) 1701.
[19] S. Gronert, J. Am. Soc. Mass Spectrom. 9 (1998) 845.
[20] H.B. Ambroz, K.R. Jennings, T.J. Kemp, Org. Mass Spectrom. 23 (1988) 605.
[21] (a) D. Zhang, R.G. Cooks, Int. J. Mass Spectrom. 195/196 (2000) 667;
(b) M.P. Ince, B.A. Perera, M.J. van Stipdonk, Int. J. Mass Spectrom. 207 (2001) 41;
(c) C. Hao, R.E. March, J. Mass Spectrom. 36 (2001) 509;
(d) D.X. Zhang, L.M. Wu, K.J. Koch, R.G. Cooks, Eur. Mass Spectrom. 5 (1999) 353;
(e) R.R. Julian, R. Hodyss, J.L. Beauchamp, J. Am. Chem. Soc. 123 (2001) 3577;
(f) P. Eichhorn, T.P. Knepper, J. Mass Spectrom. 36 (2001) 677.
[22] S. Konig, H.M. Fales, J. Am. Soc. Mass Spectrom. 10 (1999) 273.
[23] (a) M. Cygler, M. Przybylska, R.M. Elofson, Can. J. Chem. 60 (1982) 2852;
(b) K. Sasvari, H. Hess, W. Schwarz, Cryst. Struct. Commun. 11 (1982) 781;
(c) J.C. Barnes, A. Butler, L. Anderson, Acta Crystallogr. C46 (1990) 945.
[24] I.M. Cuccovia, M.A. da Silva, H.M.C. Ferraz, J.R. Pliego Jr., J.M. Riveros, H. Chaimovich, J. Chem. Soc. Perkin Trans. 2 (2000) 1896.
[25] (a) R.W. Vachet, J.A.R. Hartman, J.H. Callahan, J. Mass Spectrom. 33 (1998) 1209;
(b) B.A. Perera, M.P. Ince, E.R. Talaty, M.J. van Stipdonk, Rapid Commun. Mass Spectrom. 15 (2001) 615.
[26] D.F. McMillen, D.M. Golden, Annu. Rev. Phys. Chem. 33 (1982) 493.
[27] (a) S.E. Tichy, K.K. Thoen, J.M. Price, J.J. Ferra, C.J. Petucci, H.I. Kenttamaa, J. Org. Chem. 66 (2001) 2726;
(b) J.L. Heidbrink, K.K. Thoen, H.I. Kenttamaa, J. Org. Chem. 65 (2000) 645;
(c) K.K. Thoen, R.L. Smith, J.J. Nousiainen, E.D. Nelson, H.I. Kenttamaa, J. Am. Chem. Soc. 118 (1996) 8669.
[28] (a) H.-W. Leung, A.G. Harrison, J. Am. Chem. Soc. 101 (1979) 3168;
(b) H.-W. Leung, A.G. Harrison, J. Am. Chem. Soc. 102 (1980) 1623;
(c) W.G. Liauw, M.S. Lin, A.G. Harrison, Org. Mass Spectrom. 16 (1981) 383.
[29] F. Cacace, G. Ciranni, P. Giacomello, J. Am. Chem. Soc. 104 (8) (1982) 2258.
[30] R.A.J. O'Hair, S. Gronert, Int. J. Mass Spectrom. 195 (2000) 303.
[31] (a) E.H. White, H.M. Perks, D.F. Roswell, J. Am. Chem. Soc. 100 (1978) 7421;
(b) X. Zheng, W.A. Tao, R.G. Cooks, J. Am. Soc. Mass Spectrom. 12 (2001) 948.
[32] A. Filippi, G. Occhiucci, M. Speranza, Can. J. Chem. 69 (1991) 732.
[33] R. Caballol, J.M. Poblet, J.P. Sarasa, J. Phys. Chem. 89 (1985) 5836.
[34] R.A.W. Johnstone, D.W. Payling, Chem. Commun. 16 (1967) 826.